Università degli Studi di Padova

Dipartimento di Ingegneria dell'Informazione

Modelling and control of the braking system of the electric Polaris Ranger all-terrain-vehicle

Laureando

Nicola Geromel

Relatore

Prof. Alessandro Beghi

Correlatore

Prof. Arto Visala

Corso di Laurea Magistrale
in Ingegneria dell'Automazione

A.A. 2013/2014

8 luglio 2014

Abstract

All-terrains-vehicles (ATV) are largely used in forest working and patrolling, supporting rangers, lumberjacks and many other workers. Recently, environmental issues led to the development of electrical ATVs, that are able to provide zero emissions, more silent and cheaper operations. Thus far, these vehicles have always been driven by humans, but the last technological developments allow the implementation of self-driving and autonomous vehicles. This is an attractive possibility to help off-road workers to gain more flexibility and autonomy in their activities and an help in rescue operations as well. A crucial part in the autonomous vehicles field is the braking performance, even more important if we consider the kind of surfaces on which these vehicles are meant to go. The problem of the wheels slippage has been deeply considered for road vehicles, but few solutions and application have been implemented for off-road ones. In this final project, an introduction study in this sense is made, focusing on the brake system modelling and evaluation of some ABS solution. The vehicle in use is a Polaris Ranger.

Many slip and braking system controls have been investigated: the newest and most complex of them allow to get really high control performances and they can cope with the system modelling uncertainties. One the most promising is the sliding mode control (SMC) for its trade-off between complexity and ability to face the uncertainties. The modelling part showed us how strongly the road state can affects the braking performance and in the other side that is extremely difficult to get a detailed model of the whole braking system.

Acknoledgments

I want to thank Prof. Arto Visala and my supervisor Ville Matikainen of the Aalto University for their assistance during the writing of this thesis. I would like to give a special thanks in general to all the Automation and Systems Technology Department of the Aalto University for the kindness they reserved to me and to Prof. Beghi Alessandro and Prof. Bianchi Nicola that gave me the opportunity to carry out my thesis in Finland and spend a wonderful period in Helsinki. It has been one of the of the most intense period of my entire life, a continuous process of growth and improvement which lasted eight months.
Thanks to my family for all the sacrifices and things they have done during the years to let me reach this result. Thanks to my dad, Alfio, to be an example, he did not to let me lack anything that I needed. To my mum, Cinzia, to be always present when I needed. To my sister, Giulia, for being ready in every moment to help me.
Thanks to my old friends Luca, Marco, Moreno, Denis, Alessandro, Claudio, Mattia, Giacomo, Angelo, Erica, Giada, Giuliano, that supported me in some hard moments: even if we were thousand of kilometres far away, I felt you always very close and without you I could not have overcame some difficulties. I own you a lot.
Thanks to all the new friends and flatmates, Benat, Maria, Ignacio, Evgenia, Carlo, Tammo, Alberto, Haiko, Oliver, Alex, Noelia, Alicia, Coco, George, Erwin, Ibai, Miguel, Magdalena, Simon, Choi, Genki, Koray: you have made me feeling like in a big family since the first moment, and these months would not have been the same without you. I will carry always in my heart every single moment we spent together.
Thanks to Martina: we grew up together and even if our streets are divided now, I wish you all the best in your life.
Furthermore, a big thank you to all my classmates during the years of the

university I spent in Padova.
Thanks in general to all the people who helped and supported me in these years: each of you gave me something special.
If now I am what I am, it is only thanks to all these special people.
Thank you.

Nicola

Ringraziamenti

Voglio ringraziare il Prof. Arto Visala e Ville Matikainen della Aalto University per la loro assistenza durante la stesura di questa tesi. Vorrei dare un ringraziamento speciale, in generale, a tutti i il dipartimento di Automation and Systems Technology della Aalto University per la gentilezza che hanno riservato a me e al Prof. Alessandro Beghi e il Prof. Bianchi Nicola che mi ha dato l'opportunitá di svolgere la mia tesi in Finlandia e trascorrere un periodo meraviglioso a Helsinki. É stato uno dei periodi piú intensi di tutta la mia vita, un continuo processo di crescita e di miglioramento che é durato otto mesi.
Grazie alla mia famiglia per tutti i sacrifici e le cose che hanno fatto per me nel corso degli anni per farmi raggiungere questo risultato. Grazie a mio padre, Alfio, per essere un esempio, non mi ha mai fatto mancare nulla. A mia madre, Cinzia, per essere sempre presente quando ho avuto bisogno. A mia sorella, Giulia, una delle persone piú brillanti che conosco, sempre pronta in ogni momento ad aiutarmi.
Grazie ai miei vecchi amici Luca, Marco, Moreno, Denis, Alessandro, Claudio, Mattia, Roberto, Giacomo, Angelo, Erica, Giada, Giuliano, che mi hanno supportato in alcuni momenti difficili: anche se eravamo a migliaia di chilometri di distanza, vi ho sentiti sempre molto vicini e senza di voi non avrei potuto superre alcune difficoltá. Vi devo motissimo.
Grazie a tutti i nuovi amici e compagni, Benat, Maria, Ignacio, Evgenia, Uri, Carlo, Tammo, Alberto, Haiko, Oliver, Alex, Noelia, Alicia, Coco, George, Erwin, Ibai, Miguel, Magdalena, Simon, Choi, Genki , Koray: mi avete fatto sentire come in una grande famiglia fin dal primo momento, e questi mesi non sarebbero stati gli stessi senza di voi. Porteró sempre nel mio cuore ogni singolo momento che abbiamo trascorso insieme.
Grazie a Martina: siamo cresciuti insieme e anche se le nostre strade si sono divise ora, ti auguro il meglio nella tua vita.

Inoltre, un grande grazie a tutti i miei compagni di classe durante gli anni dell'universitá che ho trascorso a Padova.
Grazie in generale a tutte le persone che mi hanno aiutato e sostenuto me in questi anni: ognuno di voi mi ha dato qualcosa di importante.
Se ora sono quello che sono, é solo grazie a tutte queste persone speciali.
Grazie.

Nicola

Acronyms

ABS	Anti-lock Braking System
ATV	All Terrains Vehicle
BBW	Brake-By-Wire
ECU	Electronic Control Unit
EHB	Electro-Hydraulic Brake
EMB	Electro-Mechanical Brake
FMRLC	Fuzzy Model Reference Learning Control
FSMC	Fuzzy Sliding Mode Control
HAB	Hydraulic Actuated Brakes
MMAC	multiple Model Adaptive Control
NPID	Non-linear-Proportional-Integral-Derivative
PID	Proportional-Integral-Derivative
PWM	Pulse Width Modulation
SLFSMC	Self Learning Fuzzy Sliding Mode Control
SMC	Sliding Mode Control
TCS	Traction Control System
VDSC	Vehicle Dynamic Stability Control

Contents

List of Tables

List of Figures

1 Introduction

1.1 General

Since the development of the first motor driven vehicle in 1769 and the occurrence of first driving accident in 1770, engineers were determined to reduce driving accidents and improve the safety of vehicles. It is obvious that efficient design of braking systems is to reduce accidents. Security is today one of the most interesting issues in the design of a motor vehicle: just think about the ever-increasing amount of devices which a vehicle can be equipped with in order to protect the passengers in case of a crash or prevent them from occurring. In the security field, they speak about *Passive systems* when referring to the functional elements, such as air bags, seat belts safety or anti-intrusion bars in the doors, the purpose of which is to protect the passenger in case of collision. *Active safety* devices instead are those systems that allow the driver to have higher control of the vehicle in critical conditions and thus avoiding or at least reducing the potentially hazardous situations. A schematic overview of the actual technologies is presented in Figure A1 in Appendix B.
Nowadays, the importance of these systems in preventing crashes and dangerous situations is universally recognized and these devices are widely used on all

cars as standard or mandatory by law. Vehicle experts have developed the latter field (Active safety devices) through the invention of the first mechanical anti-lock-braking system (ABS) which have been designed and produced in aerospace industry in 1929. The french engineer Gabriel Voisin is often credited with developing the very first ABS version. In 1945, the first set of ABS brakes were put on a Boeing B-47 to prevent spin outs and tires from blowing and later in the 1950s, ABS brakes were commonly installed in airplanes. Soon after, in the 1960s, high end automobiles were fitted with rear-only ABS. In the 1970s, much of the rapid development of modern ABS was undertaken when Robert Bosch acquired a series of patents, and began a joint development venture with Mercedes-Benz. The birth of the first active control system in motor vehicles dates back more than thirty years ago: in 1978 the first ABS system was available for the first time as an option on the cars S-class Mercedes Benz and a short time later on the BMW 7 Series. The active safety systems have undergone a constant evolution over the years, thanks in part to the increasing availability of advanced technologies at prices relatively low. The trend exploded in the 1980s. Today, all- wheel ABS can be found on the majority of late model vehicles and even on select motorcycles. *ABS is recognized as an important contribution to road safety as it is designed to keep a vehicle steerable and stable during heavy braking moments by preventing wheel lock.* It is well known that wheels will slip and lock-up during severe braking or when braking on a slippery road surface (wet, icy, ...) . This usually causes a long stopping distance and sometimes the vehicle will lose steering stability. The objective of ABS is to manipulate the wheel slip so that a maximum friction is obtained and the steering stability (also known as the lateral stability) is maintained. That is, to make the vehicle stop in the shortest distance possible while maintaining the directional control. The ideal goal for the control design is to regulate the wheel velocity. In the following years other active safety systems have been developed, such as electronic brake distribution and traction control, as long as it has been abandoned the idea of improving the behaviour of the vehicle in some special driving situations and the designers started focusing on a overall optimization of the car dynamic behaviour. The technologies of ABS are nowadays also applied in traction control system (TCS) and vehicle dynamic stability control (VDSC).

The following chapter will present the vehicle's active control systems most used by car manufacturers with the purpose of following the evolution of these

systems and fully understanding the potential and limitations. The control logics will also be introduced as provided by the car manufacturers.

1.2 Final project outline and target

This final project belongs to a bigger project that aims to make the ATV Polaris Ranger completely autonomous. Several research groups are working together to reach the target, each of them on a specific part of the vehicle: steering, vision system, central control unit. The braking system has been my area of research. The work's target is providing an introduction to the anti-lock braking system features and characteristics and developing some mathematical models of the braking system in order to evaluate performance and providing some tools for simulations. Whenever it has been possible, the mathematical models have been implemented in Matlab/Simulink environment. In other cases, the lack of parameters and the need for some model identification made impossible to proceed with some simulations and only the theoretical model is given.

Models of the quarter of vehicle and tire-road interaction have been completed, whilst the one of the hydraulic system did not. An simplified overall model has also been built in Simulink: the idea is that this model can be a basic platform on which future works can be added.

In the appendices, a model of a fast switching solenoid valve is reported: it has been derived while trying to model the entire hydraulic brake modulator, in which the performances are strictly related to those ones of the valves, but because of the reason mentioned before, it is still incomplete. It has been reported as well, as a basis for possible future developments.

2

The Anti-lock Braking System

An anti-lock braking system (ABS) consists of a conventional hydraulic brake system plus anti-lock components which affect the control characteristics of the ABS. In general the main components are: master cylinder, hydraulic control unit (also called ECU), hydraulic pressure sensors, speed sensors, disk brakes and the brake hoses. In Figure 2.1 these components are shown in the vehicle considered in this final project.

- **1 - master cylinder**: the master cylinder is basically an hydraulic actuator that transforms the driver's braking force in pressure inside the hydraulic braking circuit. A depth discussion on how it works will be faced in the fourth chapter;

- **2 - hydraulic control unit**: this components is the core of ABS. There are many versions and different technologies, but the main purpose is to manage the braking fluid pressure inside the system, in order to get the best braking performance. To achieve this, the control unit takes in input information signals as wheel speed, acceleration, slip ratio, pressure and according to a proper control algorithm, drives the hydraulic valves and actuator to increase, maintain or decrease the pressure. More details

Figure 2.1: Anti-lock braking system components.

about this component will be given in the following chapters;

- **3 - hydraulic pressure sensors**: these sensor provide the pressure information from the master cylinder and the wheel cylinders;

- **4 - disk brakes**: nowadays, disk brakes are installed in almost all the vehicles, although some times the drum ones are still in use on the rear wheels of the smallest car models on the market. This component transforms the brake fluid pressure in a braking force pushing the pad against the metal disk. The friction slows down the wheel;

- **5 - speed sensors**: the anti-lock braking system needs some way of knowing when a wheel is about to lock up. The speed sensors, which are located at each wheel, provide this information. Even in this case, many different technologies are available on the market, according to the applications. In the automotive field, speed encoders are used the most;

- **6 - brake hoses**: the hoses, hard or flexible, bear the fluid between all the components involved in the system. The most important features are

the resistance (to avoid leaks) and the ability to avoid expansions which could introduce some delays and further dynamics in the fluid flow.

2.1 New ABS actuation technologies

Nowadays, the ABS available on most passenger cars are equipped with hydraulic brake actuators (HAB) with discrete dynamics (see Figure 2.2).
In these systems the pressure exerted by the driver on the pedal is transmitted to the hydraulic system via an inlet (or build) valve, which communicates with the brake cylinder. Moreover, the hydraulic system has a second valve, the outlet (or dump) valve, which can discharge the pressure and which is connected to a low pressure accumulator. A pump completes the overall system. The braking force acts on the wheel cylinder, which transmits it to the pads and, finally, to the brake discs. According to its physical characteristics, the HAB actuator is only capable of providing three different control actions. Increase the brake pressure: in this case the build valve is open and the dump one closed. Hold the brake pressure: in this case both valves are closed, and decrease the brake pressure: in this case the build valve is closed and the dump one open. The system however will be described with more detail in the following.
The HAB are characterised by a long life-cycle and high reliability, and this is the main motivation which has up to now prevented the new generation of braking systems (electro-hydraulic and electro-mechanical) to enter the mass production. On the other hand, the disadvantage of HAB is related to ergonomic issues: with these brakes, in fact, the driver feels pressure vibrations on

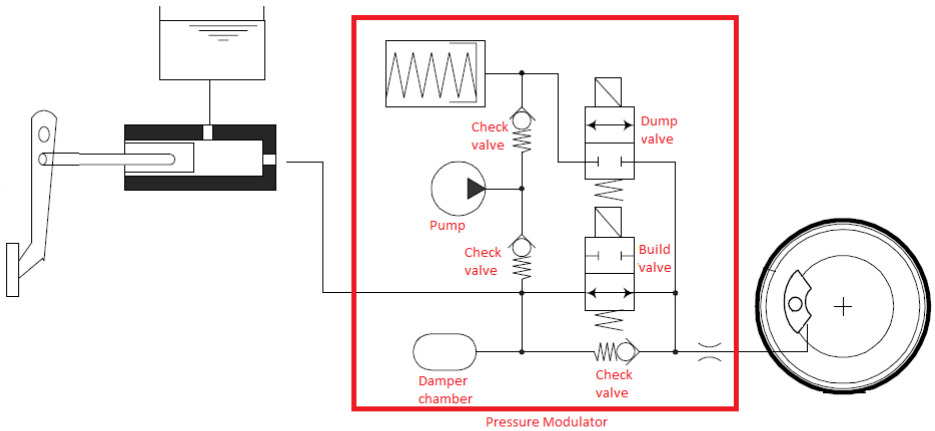

Figure 2.2: Hydraulic braking system (Figure modified from [1]).

the brake pedal when the ABS is activated, due to the large pressure gradient in the hydraulic circuit. In fact, the HAB are wired to the brake pedal, hence their action cannot bypass that of the driver, but it is superimposed onto it. The new generation of braking control systems will be based on either electro-hydraulic or electro-mechanical brakes; the latter will be the technology employed in upcoming brake-by-wire (BBW) systems. In electro-hydraulic brakes (EHB), a force feedback is provided at the brake pedal (so as to have the drivers feel the pressure they are exerting) and an electric signal measured via a position sensor is transmitted to a hydraulic unit endowed with an electronic control unit (ECU), physically connected to the caliper (i.e., the system made of the external brake body). The electro-mechanical brakes (EMB) are characterised by a completely dry electrical component system that replaces conventional actuators with electric motor-driven units. The main differences between the three actuation technologies mentioned are summarized in Table 2.1.

	HAB	**EHB**	**EMB**
Techology	Hydraulic	Electro-hydraulic	Electro-mechanical
Force modulation	Discrete (on/off)	Continuous	Continuos
Ergonomics	Pedal Vibration	No vibrations	No vibrations
Environmental issues	Toxic oils	Toxic oils	No oil

Table 2.1: Braking system actuation technologies.

With respect to the traditional brakes based on solenoid valves and hydraulic actuation, the main potential benefits of EMB are the following:

- they allow an accurate continuous adjustment of the braking force;
- no disturbances (pressure vibrations) are present on the brake pedal, even if the ABS system is active;
- the integration with the other active control systems is easier thanks to the electronic interface;
- there is a pollution reduction, as the toxic hydraulic oils are completely removed.

2.2 ABS control overview

ABS brake controllers pose unique challenges to the designer. Depending on road conditions, the maximum braking torque may vary over a wide range; the tire slippage measurement signal, crucial for controller performance, is both highly uncertain and noisy; on rough roads, the tire slip ratio varies widely and rapidly due to tire bouncing; brake pad coefficient of friction changes; the braking system contains transportation delays which limit the control system bandwidth.
ABS control is a highly a non-linear control problem due to the complicated relationship between friction and slip. Another impediment in this control problem is that the linear velocity of the wheel is not directly measurable and it has to be estimated. Friction between the road and tire is also not readily measurable or might need complicated sensors (recently some slip ratio observers have been developed in order to estimate the slip ratio [2]).
Anti-lock brake systems prevent brakes from locking during braking. Under normal braking conditions the driver controls the brakes. However, on slippery roadways or during severe braking, when the driver causes the wheels to approach lock-up, the anti-lock system takes over. ABS modulates the brake line pressure independently of the pedal force, to bring the wheel speed back to the slip level range that is necessary for optimal braking performance. An anti-lock system consists of a hydraulic modulator, wheel speed sensors, and an electronic control unit. The ABS is a feedback control system that modulates the brake pressure in response to wheel deceleration and wheel angular velocity to prevent the controlled wheel from locking. The system shuts down when the vehicle speed is below a pre-set threshold. The objectives of anti-lock systems are threefold: to reduce stopping distances, to improve stability, and to improve steerability during braking:

- **Stopping Distance**: The distance to stop is a function of the initial velocity, the mass of the vehicle, and the braking force. By maximizing the braking force the stopping distance will be minimized if all other factors remain constant. However, on all types of surfaces, there exists a peak in fiction coefficient (this issue will be presented in detail when modelling the tire-road interaction). It follows that by keeping all of the wheels of a vehicle near the peak, an anti-lock system can attain maximum frictional force and, therefore, minimum stopping distance.

- **Stability**: Although decelerating and stopping vehicles constitutes a fundamental purpose of braking systems, maximum fiction force may not be desirable in all cases. For example, if the vehicle is on surface such that there is more longitudinal friction on one side of the vehicle than on the other one,(for example one side on dry asphalt and the other on a wet surface because of a water patch on the street), applying maximum braking force on both sides will result in a yaw moment that will tend to pull the vehicle to the high friction side and contribute to vehicle instability, and forces the operator to make excessive steering corrections to counteract the yaw moment. If an anti-lock system can maintain the slip of both rear wheels at the level where the lower of the two fiction coefficients peaks , then lateral force is reasonably high, though not maximized. This contributes to stability and is an objective of anti-lock systems.

- **Steerability**: Good peak frictional force control is necessary in order to achieve satisfactory lateral forces and, therefore, satisfactory steerability. Steerability while braking is important not only for minor course corrections but also for the possibility of steering around an obstacle during the braking manoeuvre.

2.3 Anti-lock Braking System control: state of the art

Researchers have employed various control approaches to tackle this problem. A sampling of the research done for different control approaches is shown in Figure 2.3. One of the technologies that has been applied in the various aspects of ABS control is soft computing. A brief review of ideas of soft computing and how they are employed in ABS control are given below.

Classical Control

Out of all control types, the well known PID controller has been used to improve the performance of the ABS. Song, et al. [3] presented a mathematical model that is designed to analyze and improve the dynamic performance of a vehicle. A PID controller for rear wheel steering is designed to enhance the stability,

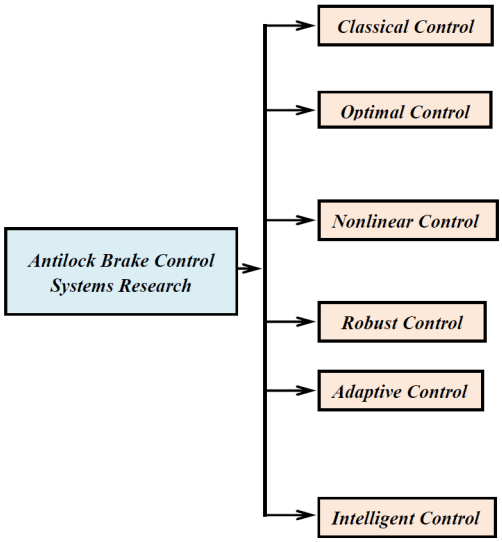

Figure 2.3: Recent technologies for ABS control.

steerability, and driveability of the vehicle during transient maneuvers. The braking and steering performances of controllers are evaluated for various driving conditions, such as straight and J-turn maneuvers. The simulation results show that the proposed full car model is sufficient to predict vehicle responses accurately. The developed ABS reduces the stopping distance and increases the longitudinal and lateral stability of both two and four-wheel steering vehicles. The results also demonstrate that the use of a rear wheel controller as a yaw motion controller can increase its lateral stability and reduce the slip angle at high speeds.

The PID controller, however, is simple in design but there is a clear limitation of its performance. It doesn't posses enough robustness for practical implementation. For solving this problem, Jiang [4] applied a new Non-linear PID (NPID) control algorithm to a class of truck ABS problems. The NPID algorithm combines the advantages of robust control and the easy tuning of the classical PID controller. Simulation results show that NPID controller has shorter stopping distance and better velocity performance than the conventional PID controller.

Optimal Control Methods Based on Lyapunov approach

The optimal control of non-linear system such as ABS is one of the most challenging and difficult subjects in control theory. Tanelli et al. [5] proposed a non-linear output feedback control law for active braking control systems. The

control law guarantees bounded control action and can cope also with input constraints. Moreover, the closed-loop system properties are such that the control algorithm allows detecting the tire-road friction without the need of a friction estimator, if the closed-loop system is operating in the unstable region of the friction curve, thereby allowing enhancing both braking performance and safety. The design is performed via Lyapunov-based methods and its effectiveness is assessed via simulations on a multibody vehicle simulator. The change in the road conditions implies continuous adaptation in controller parameter. In order to resolve this issue, an adaptive control with Lyapunov approach is suggested by R. R. Freeman [6]. Feedback linearization in combination with gain scheduling is suggested by Liu and Sun [7]. A gain scheduled LQ control design approach with associated analysis, and, except [8], is the only one that contains detailed experimental evaluation using a test vehicle. In [9], an optimum seeking approach is taken to determine the maximum friction, using sliding modes. Sliding mode control is also considered in [10] and [11]. Another non-linear modification was suggested by Ünsal and Kachroo [24] for observer-based design to control a vehicle traction that is important in providing safety and obtaining desired longitudinal vehicle motion. The direct state feedback is then replaced with non-linear observers to estimate the vehicle velocity from the output of the system (i.e., wheel velocity).

Non-linear Control Based on Backstepping Control Design

The complex nature of ABS requiring feedback control to obtain a desired system behaviour also gives rise to dynamical systems. Ting and Lin [18] developed the anti-lock braking control system integrated with active suspensions applied to a quarter car model by employing the nonlinear backstepping design schemes. In emergency, although the braking distance can be reduced by the control torque from disk/drum brakes, the braking time and distance can be further improved if the normal force generated from active suspension systems is considered simultaneously. Individual controller is designed for each subsystem and an integrated algorithm is constructed to coordinate these two subsystems. As a result, the integration of anti-lock braking and active suspension systems indeed enhances the system performance because of reduction of braking time and distance. Wang, et al. [13] compared the design process of back-stepping approach ABS via multiple model adaptive control (MMAC) controllers. The

high adhesion fixed model, medium adhesion fixed model, low adhesion fixed model and adaptive model were four models used in MMAC. The switching rules of different model controllers were also presented. Simulation was conducted for ABS control system using MMAC method basing on quarter vehicle model. Results show that this method can control wheel slip ratio more accurately, and has higher robustness, therefore it improves ABS performance effectively. Tor Arne Johansen [14] provided a contribution on non-linear adaptive back-stepping with estimator resetting using multiple observers. A multiple model based observer/estimator for the estimation of parameters was used to reset the parameter estimation in a conventional Lyapunov based non-linear adaptive controller. Transient performance can be improved without increasing the gain of the controller or estimator. This allows performance to be tuned without compromising robustness and sensitivity to noise and disturbances. The advantages of the scheme are demonstrated in an automotive wheel slip controller.

Robust Control Based on Sliding Mode Control Method

Sliding mode control is an important robust control approach. For the class of systems to which it applies, sliding mode controller design provides a systematic approach to the problem of maintaining stability and consistent performance in the face of modelling imprecision. On the other hand, by allowing the trade-off between modelling and performance to be quantified in a simple fashion, it can illuminate the whole design process. Several results have been published, [33] is an example. In these works design of sliding-mode controllers under the assumption of knowing the optimal value of the target slip was introduced. A problem of concern here is the lack of direct slip measurements. In all previous investigations the separation approach has been used. The problem was divided into the problem of optimal slip estimation and the problem of tracking the estimated optimal value. J.K. Hedrick, et al. [15], [16] suggested a modification of the technique known as sliding mode control. It was chosen due to its robustness to modelling errors and disturbance rejection capabilities. Simulation results are presented to illustrate the capability of a vehicle using this controller to follow a desired speed trajectory while maintaining constant spacing between vehicles. Therefore a sliding mode control algorithm was implemented for this application. While Kayacan [17] proposed a grey sliding-

mode controller to regulate the wheel slip, depending on the vehicle forward velocity. The proposed controller anticipates the upcoming values of wheel slip and takes the necessary action to keep the wheel slip at the desired value. The performance of the control algorithm as applied to a quarter vehicle is evaluated through simulations and experimental studies that include sudden changes in road conditions. It is observed that the proposed controller is capable of achieving faster convergence and better noise response than the conventional approaches. It is concluded that the use of grey system theory, which has certain prediction capabilities, can be a viable alternative approach when the conventional control methods cannot meet the desired performance specifications. In real systems, a switched controller has imperfections which limit switching to a finite frequency. The oscillation with the neighborhood of the switching surface cause chattering. Chattering is undesirable, since it involves extremely high control activity, and further-more may excite high-frequency dynamics neglected in the course of modelling. Chattering must be reduced (eliminated) for the controller to perform properly.

Adaptive Control Based on Gain Scheduling Control Method

Ting and Lin [18] presented an approach to incorporate the wheel slip constraint as a priori into control design so that the skidding can be avoided. A control structure of wheel torque and wheel steering is proposed to transform the original problem to that of state regulation with input constraint. For the transformed problem, a low-and-high gain technique is applied to construct the constrained controller and to enhance the utilization of the wheel slip under constraint. Simulation shows that the proposed control scheme, during tracking on a snow road, is capable of limiting the wheel slip, and has a satisfactory co-ordination between wheel torque and wheel steering.

Intelligent Control Based on Fuzzy Logic

Fuzzy Control (FC) has been proposed to tackle the problem of ABS for the unknown environmental parameters (see for example [19], [20], [21], [22]). However, the large amount of the fuzzy rules makes the analysis complex. Some researchers have proposed fuzzy control design methods based on the sliding-mode control (SMC) scheme. These approaches are referred to as fuzzy sliding-mode control (FSMC) design methods [23]. Since only one variable is

defined as the fuzzy input variable, the main advantage of the FSMC is that it requires fewer fuzzy rules than fuzzy control does. Moreover, the FSMC system has more robustness against parameter variation [24]. Although FC and FSMC are both effective methods, their major drawback is that the fuzzy rules should be previously tuned by time-consuming trial-and-error procedures. To tackle this problem, adaptive fuzzy control (AFC) based on the Lyapunov synthesis approach has been extensively studied [25]. With this approach, the fuzzy rules can be automatically adjusted to achieve satisfactory system response by an adaptive law. Lin and Hsu [26] proposed a self-learning fuzzy sliding-mode control (SLFSMC) design method for ABS. In the proposed SLFSMC system, a fuzzy controller is the main tracking controller, which is used to mimic an ideal controller; and a robust controller is derived to compensate for the difference between the ideal controller and the fuzzy controller. The SLFSMC has the advantages that it can automatically adjust the fuzzy rules, similar to the AFC, and can reduce the fuzzy rules, similar to the FSMC. Moreover, an error estimation mechanism is in-vestigated to observe the bound of approximation error. All parameters in SLFSMC are tuned in the Lyapunov sense, thus, the stability of the system can be guaranteed. Finally, two simulation scenarios are examined and a comparison between a SMC, an FSMC, and the proposed SLFSMC is made. The ABS system performance is examined on a quarter vehicle model with non-linear elastic suspension. The parallelism of the fuzzy logic evaluation process ensures rapid computation of the controller output signal, requiring less time and fewer computation steps than controllers with adaptive identification. The robustness of the braking system is investigated on rough roads and in the presence of large measurement noise. The simulation results present the system performance on various road types and under rapidly changing road conditions. While conventional control approaches and even direct fuzzy/ knowledge based approaches have been successfully implemented, their performance will still de-grade when adverse road conditions are encountered. The basic reason for this performance degradation is that the control algorithms have limited ability to learn how to compensate for the wide variety of road conditions that exist. Laynet et al. [27] and Laynet and Passino [28] introduced the idea of using the fuzzy model reference learning control (FMRLC) technique for maintaining adequate performance even under adverse road conditions. This controller utilizes a learning mechanism which observes the plant outputs and adjusts the rules in a direct fuzzy controller so that the overall system behaves like a

"reference model" which characterizes the desired behaviour. The performance of the FMRLC-based ABS is demonstrated by simulation for various road conditions and "split road conditions" (the condition where emergency braking occurs and the road switches from wet to icy or vice versa).

3

Hydraulic System Modelling

From development to deployment, models of vehicle dynamics play an essential role in all the aspects of the vehicle control simulation and design. In the context of brake control, modelling the vehicle dynamics provides a basis for hardware design and evaluation, control algorithm development and simulation.

Since automotive braking systems do not have a unique actuation point as in the throttle input in engine control, the design of brake actuators is much more difficult. Dynamic models are therefore required to match the complexity of the model and its performance. Furthermore, since the evaluation of controllers on the test track is expensive, this plant model should be able to provide an accurate simulation from which the performance can be estimated prior to experimental validation. To achieve these objectives, a good model should make control problems (like nonlinearities, disturbances, uncertainty) explicit, provides a sufficient fidelity in the simulation and be simple enough to provide a basis for model-based controllers. The reference vehicle used in this final project is the Polaris Ranger of of Figure 3.1.
The general layout of a hydraulic actuated braking system is that one of Figure 3.2.

Figure 3.1: Polaris Ranger.

The main characteristic of the HAB (hydraulic actuated brakes) type of braking system is that the driver's applied force on the brake lever is directly transmitted to the brakes by a hydraulic circuit. The driver pushes the brake pedal and the force is initially multiplied by the pedal mechanical lever ratio. In some vehicles,a second force multiplication is operated by the vacuum booster (wherever it is present, in our vehicle it is not) and finally a rod pushes the brake fluid inside the master cylinder increasing in this way the brake lines pressure.

Safety regulations require each HAB system to have two separate brake circuits, which often results in either a crossed (X) or parallel (II) configuration as shown in Figure 3.3. These configuration can prevent a complete failure of the vehicle braking system, or at least highly reducing the possibility of such an event. If one the two lines breaks down, the other one allows to stop the vehicle. The main difference between the two is that with the crossed layout (X) the vehicle keeps the lateral stability during the braking action while this could be a problem with the parallel one (II). In our vehicle, the second configuration is implemented, delivering the fluid separately between the front and rear axles.

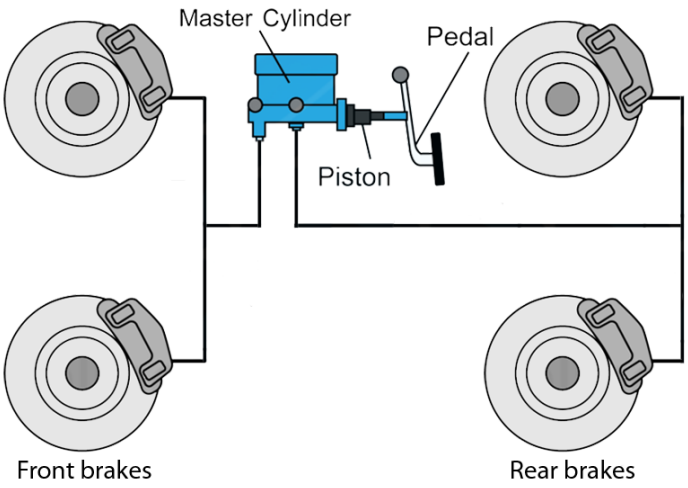

Figure 3.2: General layout of a hydraulic actuated braking system.

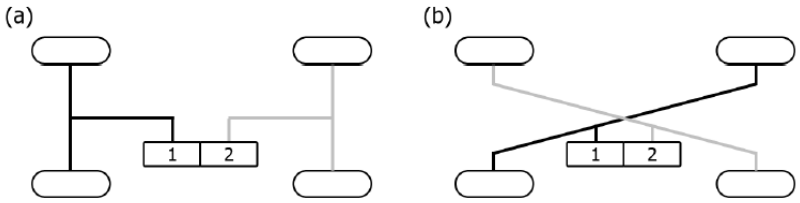

Figure 3.3: (a) II configuration (b) X configuration

3.1 Polaris Ranger's hydraulic system

The hydraulic braking system of a vehicle plays three major roles while braking, as mentioned before. First of all, it provides a force transfer and amplification between the driver's input and the actual friction element. Before the introduction of hydraulics by Deusenberg (during the 20s of the last century), this task had to be accomplished through mechanical linkages. Secondly, the design of modern hydraulic systems, with two concentric pistons in the master cylinder enhances the safety allowing some braking even in the event of failure of one circuit. Finally, the presence of the proportioning valve maintains the stability facing the weight transfer while braking, preventing in this way premature wheel lock-up.

The Polaris Ranger is equipped with a modern tandem master cylinder (see Figure 3.4) that contains primary and secondary pistons arranged concentrically in a single bore. The schematic layout is shown in Figure 3.5.

As mentioned before, the master cylinder splits into two sealed circuit the hy-

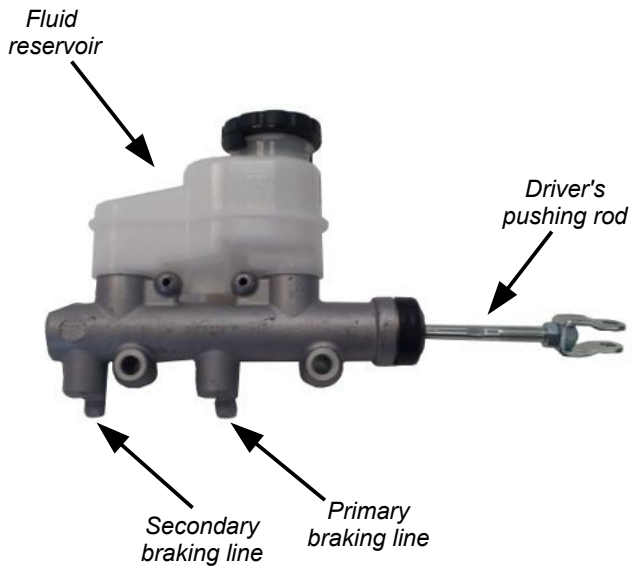

Figure 3.4: Polaris ranger tandem master cylinder.

draulic system. Each circuit is sealed with a o-ring type seal. This construction allows to split the brake hydraulics into two separate lines, one for the front wheel and the other for the rear ones (in the case of our vehicle). As previously discussed, this layout increases the vehicle safety in case of brake failure.
With reference to Figure 3.6, When the driver pushes the brake pedal, it pushes on the primary piston through a mechanical linkage. Pressure builds in the cylinder and lines as the brake pedal is depressed further. While pushing, the return spring in the primary chamber and the mechanical linkage between the primary and secondary chambers transmits the driver's force to the secondary chamber too. If the brakes are operating properly, the pressure will be the same in both circuits. The most relevant feature of the tandem master cylinder is the ability to keep the possibility to brake even in case of failure of one line. This situation is decribed in Figure 3.7.
In the first figure there is a leak in the primary line. Because of this leak the pressure inside the primary chamber does not build up and the right part of the chamber is pushed against the left one. This allows to transmit the braking input to the secondary chamber thus preventing the complete failure of the braking system. In the second figure, the leak is in the secondary line. The pressure inside the secondary chamber does not build up and the piston inside is pushed against the bottom of the tandem master cylinder body. This allows

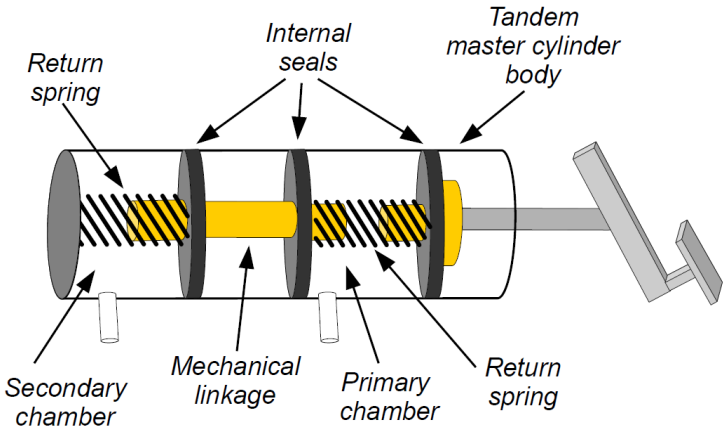

Figure 3.5: Tandem master cylinder schematic structure.

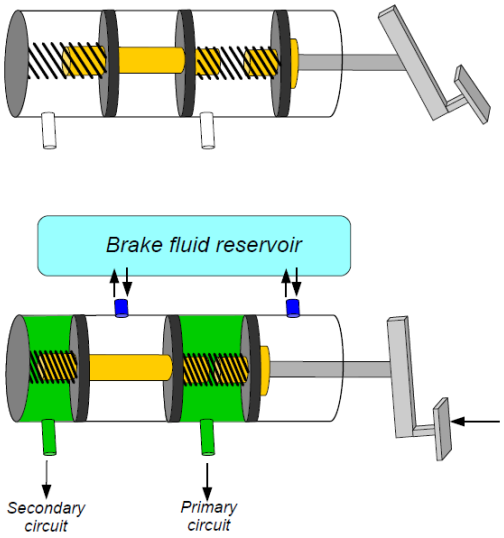

Figure 3.6: Tandem master cylinder working principles.

the increase of the pressure inside the primary chamber keeping one again the possibility to brake.

A simpler layout used in the following to derive the model is shown in Figure 3.8.

In addition, this kind of master cylinder must ensure that the brake lines remain always fulfilled of brake fluid and rid of air bubbles. At the beginning, this task was accomplished by the fluid reservoir and a couple of compensating ports (shown of Figure 3.9): by opening the brake lines to the fluid reservoir when the pedal is released, the fluid is always rid of air bubbles. With the advent of ABS technology however, this design had to be changed because the ABS

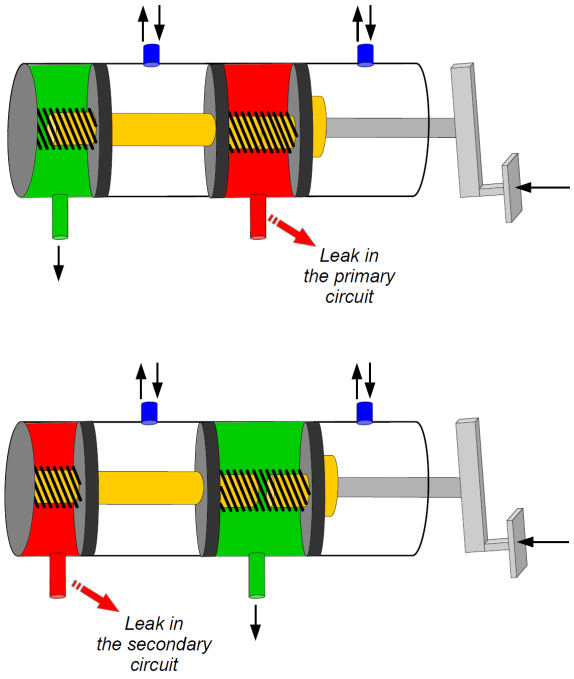

Figure 3.7: Leaks in the tandem master cylinder.

modulation pumping caused damages to the cylinder's seals.
This problem has been fixed with the introduction of the central-valve master cylinder (Figures 3.10 and 3.11). The pistons contain a small valve which opens when the pistons are pressed back again their stops in the bore and connect the brake lines to the reservoir.with this solution, even pumping the fluid pressure inside the brake lines do not damage the seals. These flow anyway, have small effects on the behaviour of brakes during braking and they will be ignored in the modelling.

The small inertias of the piston are neglected too. Under these assumptions,we consider the master cylinder consisting of two sealed hydraulic circuits which transform the driver's input force into pressure inside the brake lines. To model the hydraulic behaviour of the brake system, the following variables are considered:

- P_{mcp}: pressure inside the master cylinder primary line;
- P_{mcs}: pressure inside the master cylinder secondary line;
- $P_{w_{rf}}$: pressure inside the right front wheel cylinder;
- $P_{w_{lf}}$: pressure inside the left front wheel cylinder;

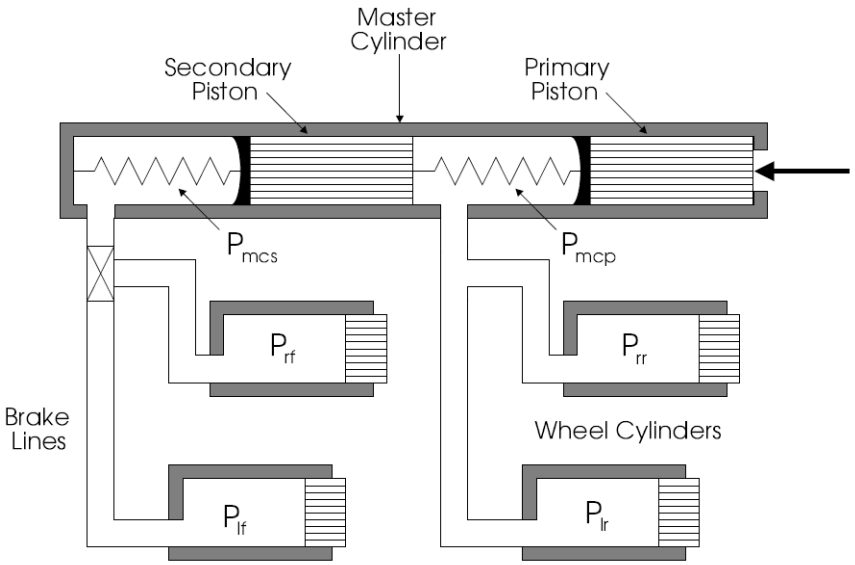

Figure 3.8: Tandem master cylinder structure.

- $P_{w_{rr}}$: pressure inside the right rear wheel cylinder;
- $P_{w_{lr}}$: pressure inside the left rear wheel cylinder;

The pressure inside the primary circuit is given by

$$P_{mcp} = \frac{(F_{pedal} - F_{p_{spring}} - F_{p_{seal}})}{A_{mc}} \tag{3.1}$$

where F_{pedal} is the driver input force, $F_{p_{spring}}$ is the primary line return spring force, $F_{p_{seal}}$ is the primary line seal friction force and A_{mc} is the master cylinder bore area. For the secondary line, the dynamic is:

$$P_{mcs} = P_{mcp} - \frac{(F_{s_{spring}} + F_{s_{seal}})}{A_{mc}} \tag{3.2}$$

with obvious meaning of the variables involved. For non-zero displacement, the return spring forces are given by:

$$F_{p_{spring}} = F_{p_{spring_0}} + K_{p_{spring}}(x_{mcp} - x_{mcs}) \tag{3.3}$$

$$F_{s_{spring}} = F_{s_{spring_0}} + K_{s_{spring}} x_{mcs} \tag{3.4}$$

where $F_{p_{spring_0}}$ and $F_{s_{spring_0}}$ are the spring pre-tensions, $K_{p_{spring}}$ and $K_{s_{spring}}$ are the spring constants and x_{mcp} and x_{mcs} are the pistons displacements in the primary and secondary line. The seal friction forces are omitted in this

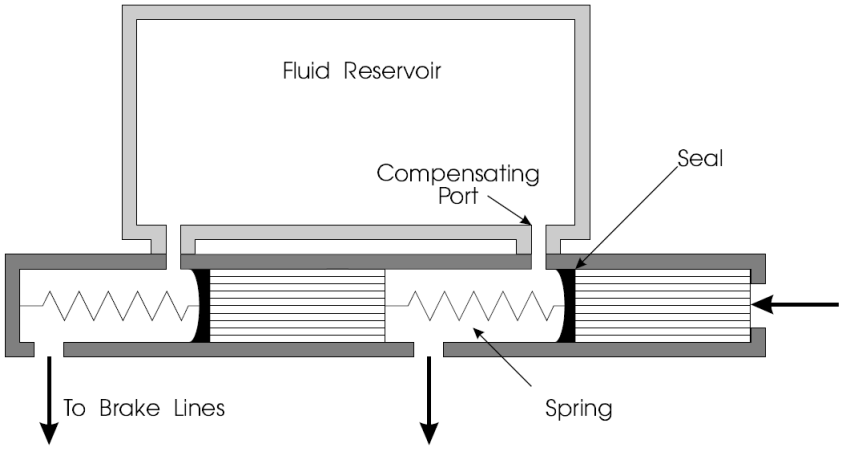

Figure 3.9: Detail of the tandem master cylinder fluid reservoir.

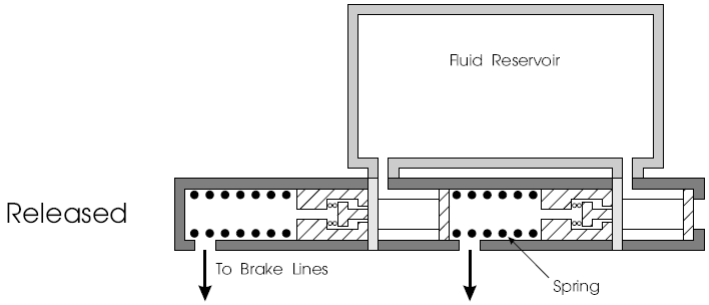

Figure 3.10: Tandem master cylinder structure.

model because of their highly non-linear behaviour and the small influence in comparison with the other forces taken into account and the brake fluid is assumed to be incompressible. Finally, the piston displacements can be computed as

$$x_{mcp} = \frac{V_{rr} + V_{lr}}{A_{mc}} + x_{mcs} \tag{3.5}$$

$$x_{mcs} = \frac{V_{rf} + V_{lf}}{A_{mc}} \tag{3.6}$$

in which V_{rr}, V_{lr}, V_{rf} and V_{lf} are the fluid displacement volume into the wheel cylinders (right rear, left rear, right front and left front respectively). In order to model the relation between the wheel pressure and the fluid displacement volume, the brake lines and wheel cylinders are assumed to have some fluid capacity: under this assumption, the pressure at each wheel is given by the

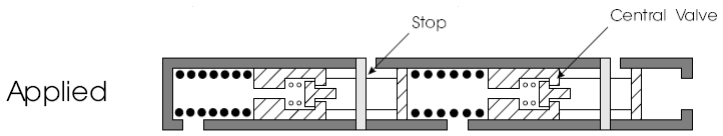

Figure 3.11: Tandem master cylinder structure.

function:

$$P_{w_{rr}} = P_{w_{rr}}(V_{rr}) \tag{3.7}$$
$$P_{w_{lr}} = P_{w_{lr}}(V_{lr}) \tag{3.8}$$
$$P_{w_{rf}} = P_{w_{rf}}(V_{rf}) \tag{3.9}$$
$$P_{w_{lf}} = P_{w_{lf}}(V_{lf}) \tag{3.10}$$
$$\tag{3.11}$$

The general shape of this function has been specified by Buschmann in 1993 and it's shown in Figure 3.12. We can notice that after an initial flow without

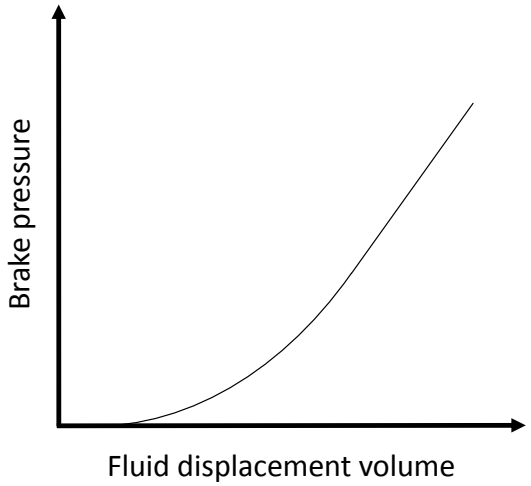

Figure 3.12: Brake fluid capacity Buschmann's shape.

pressure increase the capacity is well approximated by a linear function. The pressure increase delay in the first part of the curve is caused by the expansion of the brake lines ans seals.

Finally, thanks to the Bernoulli's equations, we can model the flow to each

wheel cylinder:

$$\dot{V_{rr}} = \sigma_{rr} C_{qrr} \sqrt{|P_{mcp} - P_{w_{rr}}|} \tag{3.12}$$

$$\dot{V_{lr}} = \sigma_{lr} C_{qlr} \sqrt{|P_{mcp} - P_{w_{lr}}|} \tag{3.13}$$

$$\dot{V_{rf}} = \sigma_{rf} C_{qrf} \sqrt{|P_{mcs} - P_{w_{rf}}|} \tag{3.14}$$

$$\dot{V_{lf}} = \sigma_{lf} C_{qlf} \sqrt{|P_{mcs} - P_{w_{lf}}|} \tag{3.15}$$

where the coefficients σ are defined as

$$\sigma_{rr} = sgn(P_{mcp} - P_{w_{rr}}) \tag{3.16}$$

$$\sigma_{lr} = sgn(P_{mcp} - P_{w_{lr}}) \tag{3.17}$$

$$\sigma_{rf} = sgn(P_{mcs} - P_{w_{rf}}) \tag{3.18}$$

$$\sigma_{lf} = sgn(P_{mcs} - P_{w_{lf}}) \tag{3.19}$$

and the parameters C_q are the flow coefficients for the brake lines.
Since in this work we are focusing on the dynamic of the quarter of car portion, we can simplify the model in order to take into account only one wheel (a front wheel) and a master cylinder with only one output line. The pressure inside the master cylinder is thus given by

$$P_{mc} = \frac{F_{pedal} - F_{spring} - F_{seal}}{A_{mc}} \tag{3.20}$$

The return spring force is defined in this case as

$$F_{spring} = F_{spring_0} + K_{spring} x_{mc} \tag{3.21}$$

in which F_{spring_0} is the master cylinder spring pre-tension. The master cylinder piston displacement is

$$x_{mc} = \frac{V}{A_{mc}} \tag{3.22}$$

where V is the volume of the displaced brake fluid. The volume variation is once again given by the Bernoulli's equation:

$$\dot{V} = \sigma C_q \sqrt{|P_{mc} - P_{wc}|} \tag{3.23}$$

where $\sigma = sgn(P_{mc} - P_{wc})$ and C_q is the fluid coefficient. The wheel cylinder pressure is again dependent on the fluid displacement: $P_{wc} = P_{wc}(V)$.
The physical parameters for the vehicle are collected in Table **??**.

Name	**Symbol**	**Value**	**Unit**
Master cylinder piston area	A_{mc}	4.91×10^{-4}	m^2
Wheel cylinder piston area	A_{wc}	7.07×10^{-4}	m^2
Master cylinder spring pre-tension	F_{spring_0}	138	N
Master cylinder spring constant	K_{spring}	175	N/m
Seal friction force	F_{seal}	80	N
Flow coefficient	C_q	1.4×10^{-6}	$\frac{m^3}{s\sqrt{kPa}}$

Table 3.1: Parameters of the Polaris Ranger braking system.

3.2 Hydraulic Actuator

Hydraulic actuated brake (HAB) uses brake fluid to apply brake pressure to pads or shoes (when drum brakes are in use). As discussed briefly before, the main parts of this system are a chamber called a master cylinder, which is located near the brake pedal; at least one wheel cylinder at each wheel (on high performance vehicles, modern disk brakes have more than one cylinder per caliper); tubes called brake pipes, which connect the master cylinder to the wheel cylinders. The cylinders and brake pipes are filled with brake fluid. Inside the master cylinder, there is a piston, which can slide back and forth. In a simple hydraulic system, the brake pedal controls this piston by means of a rod or some other mechanical links. When the driver pushes on the pedal, the piston inside the master cylinder exerts pressure on the fluid and slides forward a short distance. The fluid transmits this pressure through the brake pipes, forcing pistons in the wheel cylinders to move forward. As the wheel cylinders move forward, they apply brake pressure to pads or shoes.
The target of the anti-lock braking system, as discussed deeply in the previous chapter, is to avoid the wheel lock up and the way to reach this goal is managing the fluid pressure inside the braking lines. The set of components that carry out this task is called Hydraulic Modulator (see Figure 3.13). In this scheme, the

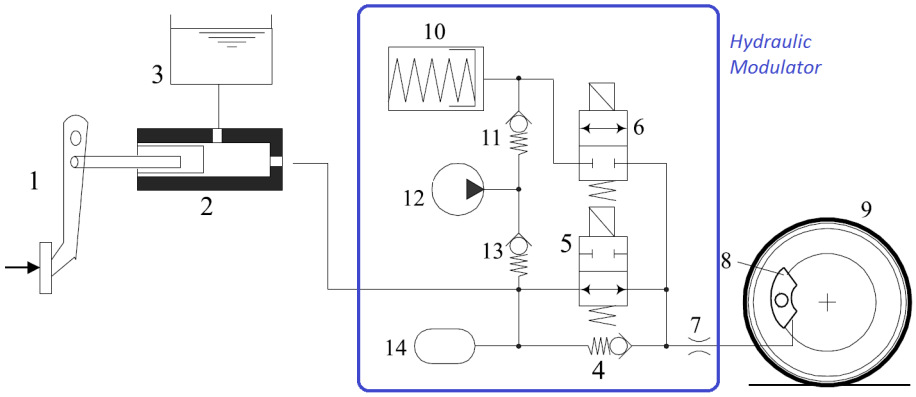

Figure 3.13: HAB anti-lock braking control layout.

driver pushes the pedal (1) when he wants to slow down the car. The forward movement of the rod causes an increase of the fluid pressure inside the master cylinder (2). Just above the master cylinder there is a fluid tank (3) that allows to release the fluid pressure inside the master cylinder and keeps the braking fluid almost free of air bubbles. The Hydraulic Modulator, is responsible for

the increase, release and holding the fluid pressure. Usually it is composed by an inlet (build) valve (5) and an outlet (dump) Valve (6): the first one, when opened, connects the master cylinder with the wheel cylinder, the latter allows the braking fluid to flow from the wheel cylinder to the low-pressure tank (10). Three check valves are present (7, 11 and 13), they ensure the proper direction for the fluid flow. Finally an hydraulic pump (12) fetches the low-pressure fluid from the low-pressure tank .
The dynamic of such modulator is quite complex but the governing equation can be written. The complete model, however, can not be completed because some parameters identification should be done in order to get the proper values for the system coefficients (this can be done when the required hardware will be installed on the vehicle). In this work, a simpler model for the hydraulic modulator is built. A similar work has been done in [41]. Here some system identification work of the hydraulic dynamics model in the laboratory is presented. They also use a simplify model low pass filter, and the identified results of these two models almost the same, so we can simplify the dynamics into a low pass filter. A rough identification of the characteristics gives a pure time delay $\tau = 7\,ms$, a pressure rate limit between $r_{max} = +750\,bar/s$ and $r_{min} = -500\,bar/s$ and a second order dynamics with a cut-off frequency of $60\,Hz$ and a damping coefficient $\xi = 0.33$.

ABS control algorithms

Manufacturers of ECU ABS/ESP (where ECU stands for Electronic Control Unit) still keep secret the control logic of electronic control units (ECU) and are limited to broadly describe their general idea, absolutely not getting into detail. In this paragraph, we will report briefly the few information available in the literature ([29], [30], [31] and [32]).
Through the modulation of the pressure in the brake's calipers, the ABS system must be able to control the longitudinal dynamics of the vehicle. The ABS's pressure dynamic is composed by three steps called *growth*, *maintenance* and *decrease*. In Figure 3.14 is depicted the typical profile of the slip-friction curve.

It is clear that to get the best braking performance for the wheel the control system should work in order to keep the wheel slip value close to the peak. To reach this target , the ABS estimates the wheel slip ratio through the angular

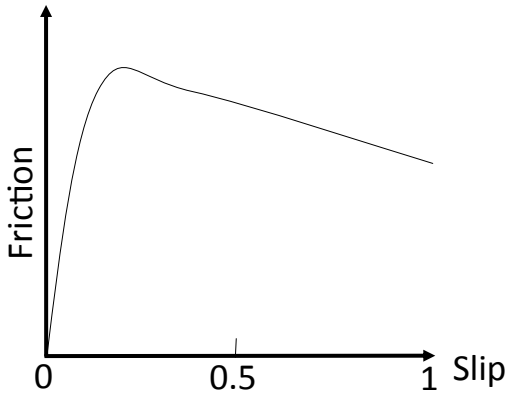

Figure 3.14: Tipical slip-friction curve.

rate sensors and controls it so that each wheel is always in the desired part of the friction curve. To compute the slip value on the wheel is therefore crucial to estimate the longitudinal velocity of the vehicle in all driving conditions. The longitudinal velocity of the vehicle is estimated as an average value between the speed of the two wheels belonging to the same diagonal, for example the left front wheel and the right rear one. It will therefore have two reference speeds, calculated independently on the two diagonals : between these two velocities ABS system always chooses the greatest in braking situations. Since a locked wheel can not be considered in the algorithm of calculation correctly , the system always checks that the deceleration of the wheel does not exceed a specified value and that the peripheral speeds of the same wheel isn't lower than the reference speed. The occurrence of one between the two conditions leads to consider the wheel close to instability.
The functional scheme of the ABS system is shown in Figure **??**. Sensor installed on the vehicle collect data in order to provide them to the control algorithm. These data are the linear velocity of the vehicle, the wheel angular velocity and the tire-road characteristic function (that is not directly accessible but has to be estimated based on the slip ratio value and on a prior knowledge about the road condition). The output of the control algorithm acts on the actuation valve in order to set the proper hydraulic pressure.

Bosch algorithm

The Bosch ABS system is used on many passenger cars. The algorithm is based on wheel spin acceleration and a critical tire slip threshold. Upon brake

pressure application, once ABS is invoked (i.e., the thresholds are exceeded), the current brake pressure application is divided into eight phases (see Figure 3.15). **Phase 1**: Initial application. Output pressure is set equal to input

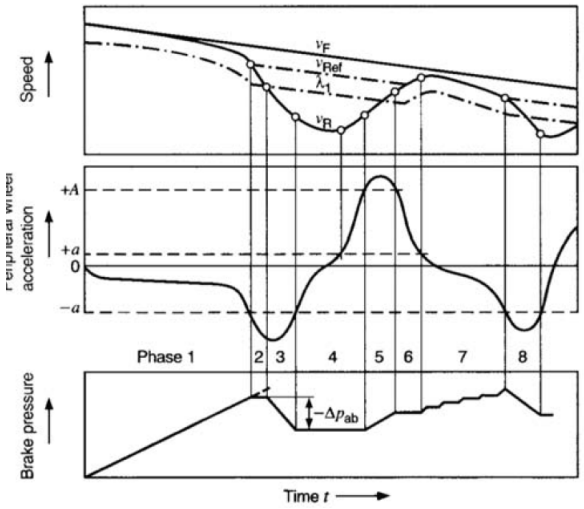

Figure 3.15: Bosch algorithm logic.

pressure. This phase continues until the wheel angular acceleration (negative) drops below the Wheel Minimum Spin Acceleration, -a.

Phase 2: Maintain pressure. Output pressure is set equal to previous pressure. This phase continues until the tire longitudinal slip exceeds the slip associated with the Slip Threshold. At this time, the current tire slip is stored and used as the slip threshold criterion in later phases. This slip corresponds to the maximum slip; the tire is beginning to lock.

Phase 3: Reduce pressure. Output pressure is decreased according to the Release Rate until the wheel spin acceleration becomes positive (this is a slight modification to the sequence shown in Figure 3.15, in which the pressure is decreased until the spin acceleration exceeds -a).

Phase 4: Maintain pressure. Output pressure is set equal to the previous pressure for the specified Apply Delay, or until the wheel spin acceleration (positive) exceeds +A, a multiple (normally 10 times) of the Wheel Maximum Spin Acceleration, +a, (signifying the wheel spin velocity is increasing at an excessive rate).

Phase 5: Increase pressure. Output pressure increases according to the Primary Apply Rate. This phase continues until the wheel spin acceleration drops and again becomes negative (this is a slight modification to the sequence shown in Figure 3, in which the pressure is increased until the spin acceleration drops

below +A).
Phase 6:Maintain pressure. Output pressure is set equal to previous pressure for the specified Apply Delay, or until wheel angular acceleration again exceeds the Wheel Minimum Wheel Spin Acceleration (negative).
Phase 7:Increase pressure. Output pressure increases according to the Secondary Apply Rate, normally a fraction (1/10) of the Primary Apply Rate. This achieves greater braking performance while minimizing the potential for wheel lock-up at tire longitudinal slip in the vicinity of peak friction. This phase continues until wheel angular acceleration drops below the Wheel Minimum Angular Acceleration (negative), indicating wheel lock-up is eminent.
Phase 8: Reduce pressure. At this point an individual cycle is complete, the process returns to Phase 3 and a new control cycle begins.
Each of the above phases begins with a comparison between the current tire longitudinal slip and the value stored during Phase 2. If the current slip exceeds this value, the normal logic is bypassed and resumed at Phase 3. This effectively allows the algorithm to .learn. the wheel slip associated with wheel lock-up on the current surface. This is referred to as .adaptive learning., and is a key to the success of this ABS algorithm. As the tire travels onto surfaces with differing friction characteristics, the ABS model is able to maximize its performance accordingly.

3.3 Disk brake braking torque

As discussed before the Polaris Ranger considered in this final project mounts four disk brakes. In Figure 3.16 is presented the general structure.
When the pressure inside the wheel cylinder increases, the wheel piston rod pushes the pad against the disk and the friction between pad and disk slows down the wheel that is rotating with the disk.
In Figure 3.17 the mathematical model used for the brake torque T_b calculation is depicted.

For this kind of braking system, the braking torque acting on a wheel can be simply defined as

$$T_b = F_{friction} r_e f f \tag{3.24}$$

where $F_{friction}$ is the friction force generated at the contact interface and r_{eff} is the effective pad radius. However friction force is dependent upon normal

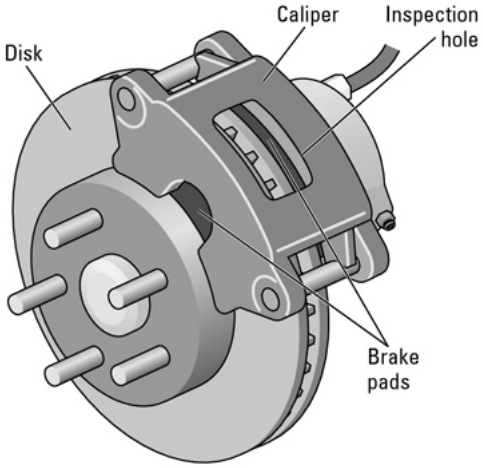

Figure 3.16: disk-brake-diagram

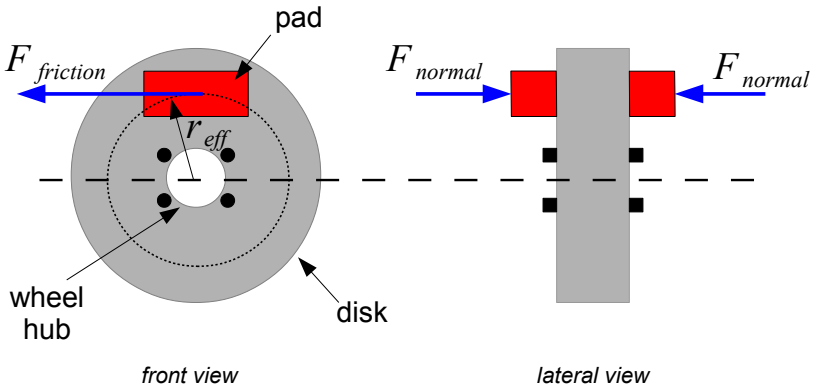

Figure 3.17: Disk brake mathematical model.

force F_{normal} and brake pad friction coefficient γ according to

$$F_{friction} = \gamma F_{normal} \tag{3.25}$$

The normal force pushing the pad against the disk is proportional to the brake cylinder pressure P_{wc} and its cross area A_{wc}:

$$F_{normal} = P_{wc} A_{wc} \tag{3.26}$$

This leads to the equation for the braking torque T_b:

$$T_b = F_{friction} r_{eff} \tag{3.27}$$
$$= \gamma F_{normal} r_{eff} \tag{3.28}$$
$$= \gamma P_{wc} A_{wc} r_{eff} \tag{3.29}$$

where A_{wc} is the wheel brake piston cross area and P_wc is, as stated in the previous section, the braking pressure generated by the hydraulic fluid inside the wheel cylinder. For a disc brake system there is a pair of brake pads, thus the total brake torque is:

$$T_b = 2\gamma P_{wc} A_{wc} r_{eff} \tag{3.30}$$

Once the brake disc is fixed, the values r_{eff} and A_{wc} are constant, while the brake pad friction coefficient γ is changing during braking depending on several factor, as the brake temperature, the sliding speed between pad and disk and the brake cylinder pressure. In general, the efficiency will increase with the temperature, up to a certain level where fading starts and friction drops rapidly. Some studies have been carried out about the behaviour of the friction coefficient γ respect the variation of the sliding speed and the pressure. The conclusions tell that the dependency is highly non linear but the friction value does not change significantly, always in the range $[0.3 - 0.5]$. This allows us to consider the friction almost constant during braking: in the rest of the work we will use the value $\gamma = 0.4$.

One more detail could be considered: as long as the pressure inside the wheel cylinder is low, the pad is not pushed out. This happens only when the pressure overcome a pressure threshold called push-out pressure $P_{pushout}$. Physically, this pressure corresponds to the force needed to overcome the caliper seal rollback. However, the push-out pressure is not available in this work. The model would be modified as follow:

$$T_b = \begin{cases} 2\gamma P_{wc} A_{wc} r_{eff} & \text{if } P_{wc} \geq P_{pushout} \\ 0 & \text{otherwise.} \end{cases} \tag{3.31}$$

This relation is implemented in Simulink as shown in Figure 3.18

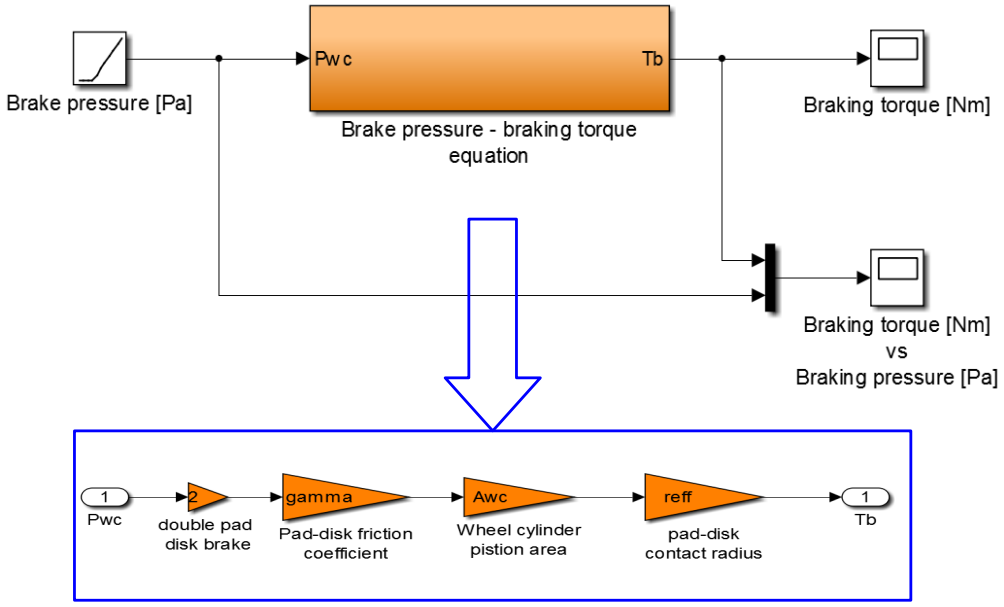

Figure 3.18: Simulink implementation of the brake pressure-torque relation.

The parameters used are given below in Table 3.2.

Name	Symbol	Value	Unit
Pad-disk friction coefficient	γ	0.4	
Wheel cylinder piston's area	A_{wc}	9.6211×10^{-4}	m^2
effective pad radius	r_{eff}	0.115	m

Table 3.2: Parameters of the brake pressure-torque model.

4

Tire-road Interaction

Forces and moments from the road act on each tire of the vehicle and highly influence the dynamics of the vehicle. This section focuses on mathematical modelling in order to describe these forces.

Unlike a rigid undeformable wheel, the tire does not make contact with the road at just one point, instead, as shown in Figure 4.1, the tire on a vehicle deforms due to the vertical load on it and makes the contact with the road over a non-zero footprint area called the contact patch.

The force the tire receives from the road is assumed to be at the center of the contact patch and can be decomposed along three orthogonal force vectors, F_z, F_x and F_y, as shown in Figure 4.2.

F_z is dependent on the load on the tire, while F_x and F_y are both dependent on several different factors as for instance road surface, tire pressure, vehicle load, longitudinal wheel slip, slip angle and camber angle. Longitudinal force F_x allows the vehicle to brake, whilst lateral force F_y ensures steerability.

In general, because of tire deformation and because of traction and braking forces exerted on the tire, the wheel ground contact point velocity v is not equal to the product ωr, as shown in Figure 4.3.

Denoting by the velocity of a pure rolling wheel whose radius is r and angular

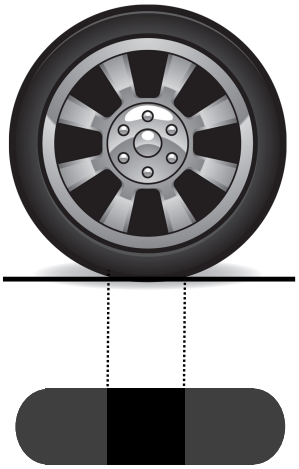

Figure 4.1: The contact patch of a tire.

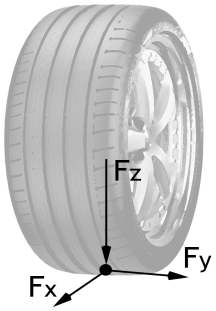

Figure 4.2: Forces acting on the tire-road contact point.

velocity is ω, the longitudinal slip coefficient λ can be defined as

$$\lambda = \frac{v - \omega r \, cos(\alpha_t)}{max\{v, \omega r \, cos(\alpha_t)\}} \tag{4.1}$$

where α_t is the wheel slip angle. In vehicle dynamics, side-slip angle is the angle between a rolling wheel's actual direction of travel and direction towards which is pointing. During the study of braking systems usually straight line braking is assumed ($\alpha_t = 0$), which simplifies modelling significantly without degrading quality of the representation. Under this assumption, the previous equation becomes:

$$\lambda = \frac{v - \omega r}{max\{v, \omega r\}} = \frac{v - \omega r}{v} \tag{4.2}$$

with $\lambda \in [0, 1]$. In particular $\lambda = 0$ corresponds to a pure rolling wheel and $\lambda = 1$ to a locked wheel. The capability of the wheel to tract is dependent on the slip ratio and the trend is shown in Figure 4.4.

It is not difficult to figure out that there is this dependence of the longitudinal

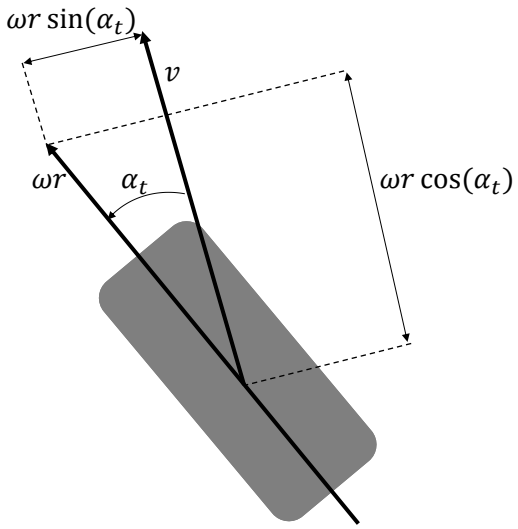

Figure 4.3: Wheel side slip angle.

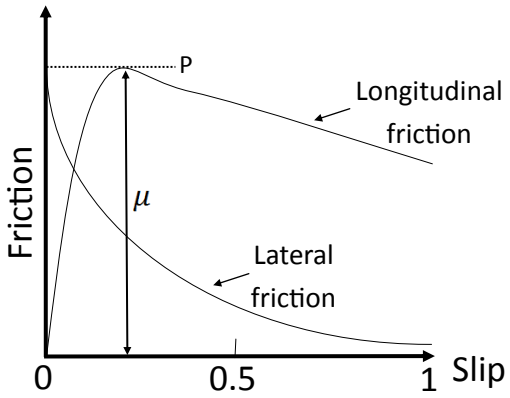

Figure 4.4: Slip-friction curve.

tire force F_x on the slip ratio λ: the friction coefficient μ is related to the capability of the tire to transform the vertical load and the sum of torques acting on it in a longitudinal force. As higher as the friction coefficient is as higher will be the corresponding longitudinal force.

From Figure 4.4 we can see that the friction coefficient reaches the maximum value at the peak value point P. When the slip ratio is below point P, the slip ratio can increase the friction. Once the slip ratio exceeds P, the traction force will decrease as a result of the decrease of adhesive coefficient. In addition to the tractive forces, the wheel must also generate a lateral force to direct the vehicle. Like the tractive forces, the lateral force is also dependent on the slip ratio. The lateral force will be decreased as the slip is increased. Thus, the steering ability will be decreased as the slip is increased. This physical phenomenon

is the main motivation for ABS brakes, since avoiding high longitudinal slip values will maintain high steerability and lateral stability of the vehicle during braking.
In straight line braking F_y is logically assumed to be 0, while the longitudinal tire force F_x can be described by:

$$F_x(\lambda, F_z) = F_z \mu_x(\lambda) \tag{4.3}$$

where μ_x is a friction function dependent on longitudinal slip λ. We focus on the fact that the longitudinal tire force depends linearly on vertical load F_z and non-linearly on the slip ratio.
There are static models as well as dynamic models to describe the longitudinal tire force. One of the best model in literature is the **Pacejka's Magic Formula** model, which is valid both for small and large slip ratios. The Magic Formula (Pacejka and Bakker, 1993) provides a method to calculate lateral and longitudinal tire forces F_y and F_x for a wide range of operating conditions, including combined lateral and longitudinal force generation. In the simpler case where only either lateral or longitudinal force is being generated, the force y can be expressed as a function of the input variable x as follow:

$$y(x) = Dsin\Big[C\, arctan\big\{Bx - E(Bx - arctan\, Bx)\big\}\Big]$$

where y is the output variable (lateral or longitudinal force) and x is the input variable (usually the slip ratio defined before). The model's parameters B,C,D,E have the following nomenclature:

- B stiffness factor;
- C shape factor;
- D peak value;
- E curvature factor.

Although this empirical formula is capable of producing characteristics that closely match measured curves for the lateral force F_y and the longitudinal one F_x, actually the function is pretty complex and the parameters specified have to be determined for the particular wheel in use and this task is particularly hard. A simpler way to carry out the model is given below.

One other simple and widespread model in literature for the friction coefficient is the Burckhardt's model, which has been derived heuristically from experimental data:

$$\mu_x(\lambda;\theta_r) = \Big[\theta_{r1}\big(1 - e^{-\lambda\theta_{r2}} - \lambda\theta_{r3}\big)\Big]e^{-\theta_{r4}\lambda v}$$

in which the vector θ_r has four parameters that are specified for different road surfaces. By changing the values of these four parameters, many different tire-road friction conditions can be modelled. The presented equation could also be used for a dynamic road surface variation. The meaning of these coefficients are:

- θ_{r1} is the maximum value of friction curve;
- θ_{r2} is the friction curve shape;
- θ_{r3} is the friction curve difference between the maximum value and the value at $\lambda = 1$;
- θ_{r4} is the wetness characteristic value and is in the range $[0.02 - 0.04]\ s/m$

In Table 4.1 the parameters are given for several kinds of road furface.

Surface Conditions	θ_{r1}	θ_{r2}	θ_{r3}
Asphalt, dry	1,029	17,16	0,523
Asphalt, wet	0,857	33,822	0,347
Concrete, dry	1,1973	25,168	0,5373
Cobblestone, dry	1,3713	6,4565	0,6691
Cobblestone, wet	0,4004	33,708	0,1204
Snow	0,1946	94,129	0,0646
Ice	0,05	306,39	0

Table 4.1: Friction parameters for the Burckhardt's tire model.

In Figure 4.5 the shapes of $\mu_x(\lambda;\theta_r)$ in different road conditions are shown. Observing Figure 4.5, one can notice that the friction trend is almost flat in the cases of snow or ice while with other surfaces it presents a rising behaviour at the beginning and a decreasing one when λ grows over $0.2 - 0.3$. This suggests the idea to achieve the best braking performance i.e. controlling the wheel behaviour in order to keep the slip ratio λ in the range in which it gives the maximum friction coefficient μ, even if the friction peak is obtained in correspondence of different slip values for different surfaces. Incidentally, the last observation reminds to a big problem of the ABS: the surface condition

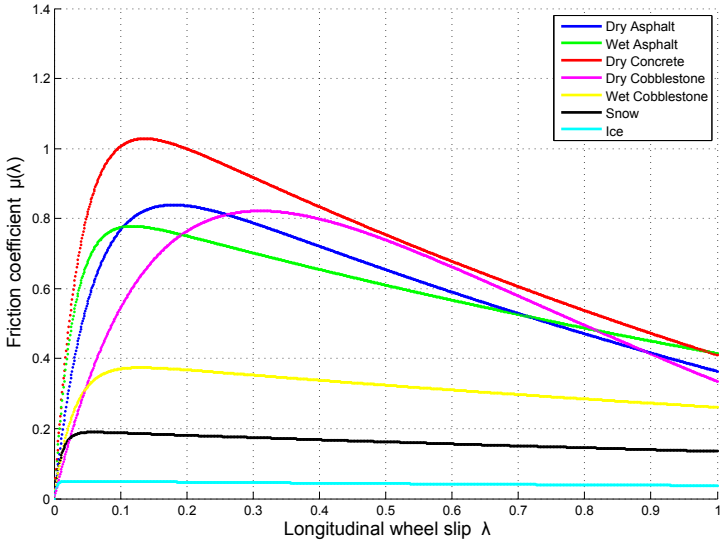

Figure 4.5: Tire-road friction on different surfaces for $v = 10\,m/s$.

can change quite fast while driving or they can even be different between the two sides of the vehicle.

From here over, for simplicity, we will omit the dependency of the friction coefficient on θ_r and we will refer to the function $\mu_x(\lambda, \theta_r)$ simply as $\mu_x(\lambda)$ or even $\mu(\lambda)$ when it is clear the reference to the longitudinal slip behaviour.

Once evaluated the behaviour of the friction coefficient μ, it is possible to determinate the longitudinal force F_x exerted by the tire on the road surface. In this project the Polaris Ranger vehicle on use weights $M_t = 1400\,kg$, taking into account the maximum load and an average driver's weight of about $80\,kg$. This means that on the single wheel, there is a load of $m = 350\,kg$. Recalling equation 4.3 and the fact that the vertical load F_z is $F_z = mg$ where g is the gravity, the interaction between the slip ratio value and the longitudinal force is shown in figure 4.6.

Looking at Figure 4.6 we can notice the big difference that arises when braking on different road surfaces: the highest braking performances are achievable on the dry concrete (over $3500\,N$ of longitudinal force) while on the ice the maximum longitudinal force is about $170\,N$. It is also remarkable that on low adherence surfaces like snow and ice, the longitudinal force trend is almost flat respect to the slip ratio, while in other surfaces the force presents a peak and then it decreases.

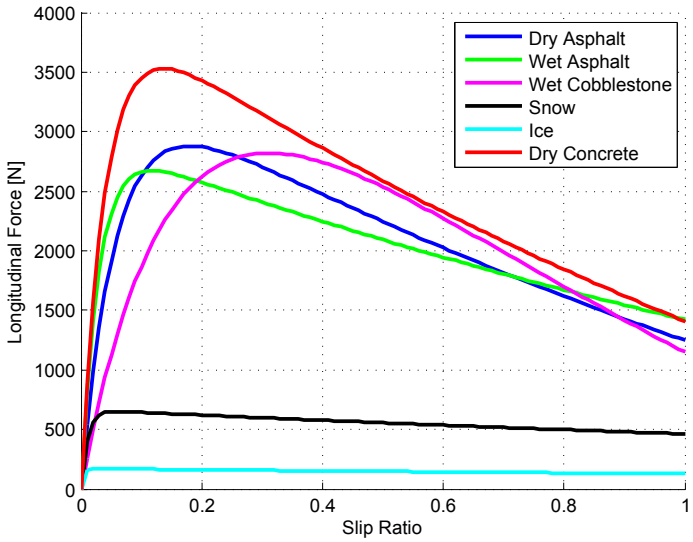

Figure 4.6: Longitudinal forces on different surfaces for $v = 10\,m/s$.

5

Quarter of Car Model

For the preliminary design and testing of braking control algorithms, a simple but effective single-corner car model (also called quarter-car model) is typically used. The model consists of a single wheel attached to a mass m (see Figure 5.1).

As the wheel rotates, driven by inertia of the mass m in the direction of the velocity v, a tyre reaction force F_x is generated by the friction between the tyre surface and the road surface. The tyre reaction force will generate a torque that initiates a rolling motion of the wheel causing an angular velocity ω. A brake torque applied to the wheel will act against the spinning of the wheel causing a negative angular acceleration. With reference to Figure 5.1 and according to Newton's second law, the dynamics of the quarter-car braking model can be represented by the following equations:

$$\begin{cases} J\dot{\omega} = rF_x - T_b \\ m\dot{v} = -F_x \end{cases} \tag{5.1}$$

where $\omega\,[rad/s]$ is the angular speed of the wheel, $v\,[m/s]$ is the longitudinal speed of the vehicle body, $T_b\,[Nm]$ is the braking torque, $F_x\,[N]$ is the longi-

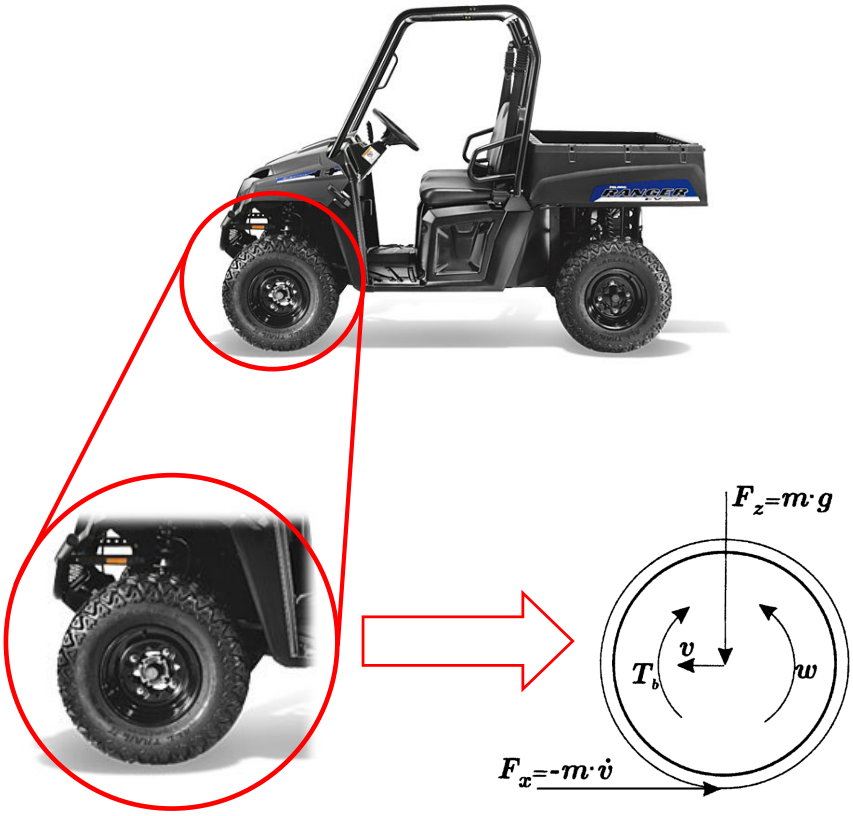

Figure 5.1: Quarter of car model.

tudinal tire-road contact force, $J\,[Kgm^2]$ $m\,[Kg]$ and $r\,[m]$ are the moment of inertia of the wheel, the quarter-car mass, and the wheel radius, respectively. Let's recall from the previous section that the longitudinal traction force F_x is given by

$$F_x(\lambda, F_z) = F_z \mu_x(\lambda)$$

and that the vertical load can be simply described as $F_z = mg$. Recalling that the slip ratio is defined as

$$\lambda = \frac{v - \omega r}{v}$$

we obtain:

$$F_x = mg\mu(\lambda, \theta_r) \;=\; mg\mu\Big(\frac{v - \omega r}{v}, \theta_r\Big) \tag{5.2}$$

By plugging equation 5.2 into equation 5.1, we finally obtain the following expression of the quarter-car model:

$$\begin{cases} J\dot{\omega} = rmg\mu\Big(\frac{v-\omega r}{v}, \theta_r\Big) - T_b \\ m\dot{v} = -mg\mu\Big(\frac{v-\omega r}{v}, \theta_r\Big) \end{cases} \tag{5.3}$$

In this last form, the state variables of the system are ω and v but since ω, v and λ are linked by the algebraic relationship 4.2 it is possible to replace the state variable ω with λ. This can be obtained by plugging the following two relationships

$$\dot{\lambda} = -\frac{r}{v}\dot{\omega} + \frac{r\omega}{v^2},\ \omega = \frac{v}{r}(1-\lambda)$$

into the first equation of 5.3, resulting in

$$\begin{cases} \dot{\lambda} = -\frac{1}{v}\left(\frac{1-\lambda}{m} + \frac{r^2}{J}\right)mg\mu(\lambda) + \frac{r}{Jv}T_b \\ m\dot{v} = -mg\mu(\lambda) \end{cases} \tag{5.4}$$

where we can delete the mass m on both sides of the second equation, obtaining the final expression for the model

$$\begin{cases} \dot{\lambda} = -\frac{1}{v}\left(\frac{1-\lambda}{m} + \frac{r^2}{J}\right)mg\mu(\lambda) + \frac{r}{Jv}T_b \\ \dot{v} = -g\mu(\lambda) \end{cases} \tag{5.5}$$

The proposed model is implemented in Simulink as shown in Figure 5.2. The

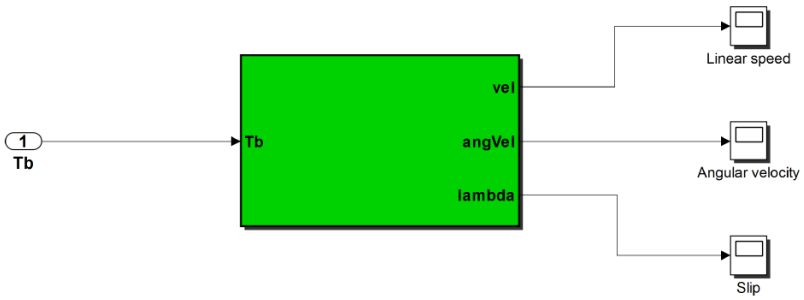

Figure 5.2: Simulink implementation of the wheel model.

input to the model is the braking torque T_q and the outputs are the wheel linear and angular speeds and the slip ratio. In Figure 5.3 there is a detailed view. In the block "Tire-road friction" is computed the friction coefficient between the tire and the road surface, based on the road condition (that are specified a priori in the Matlab script), the slip value (computed in the block named "Slip Ratio Calculation") and the linear speed of the vehicle. In order to get the linear and angular velocities, a bounded integration block is used. The initial condition specified are the initial linear velocity of the vehicle (v_0) and the angular one ($\omega_0 = \frac{v_0}{r}$). To avoid numeric problems, i.e dividing by zero,

the simulation stops when the linear velocity is $0.1\,m/s$.

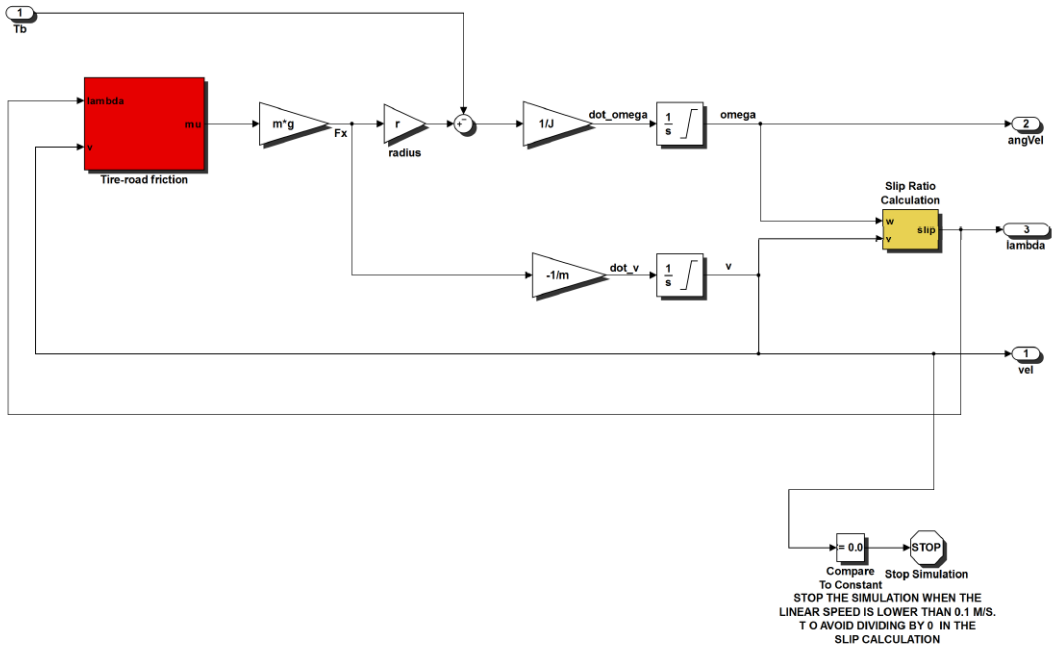

Figure 5.3: Detail of the Simulink implementation of the wheel model.

In the rest of the final project the values collected in Table 5.1 for the above parameters will be employed in numerical examples and simulations. These

Name	Symbol	Value	Unit
mass of the quarter-car model	m	350	kg
wheel inertia moment	J	1	kgm^2
wheel radius	r	0.2	m
gravity acceleration	g	9.81	m/s^2
initial linear speed	v_0	11	m/s

Table 5.1: Quarter of car model parameters of the vehicle in use.

parameters are taken from the Polaris webpage. The value of the initial linear speed v_0 in particular is set to be $11\,m/s$ because that is the maximum speed linear speed of the vehicle ($40\,km/h$).
The performance of the discussed model are presented below for the six different road conditions. All the simulations are executed with a test braking torque of $450\,Nm$ and are 2 second long. In Figure 5.4 the linear speed is shown. The initial linear speed for all the simulation is $11\,m/s$. The simulations shows that the best performance are achieved on the dry concrete, on which the

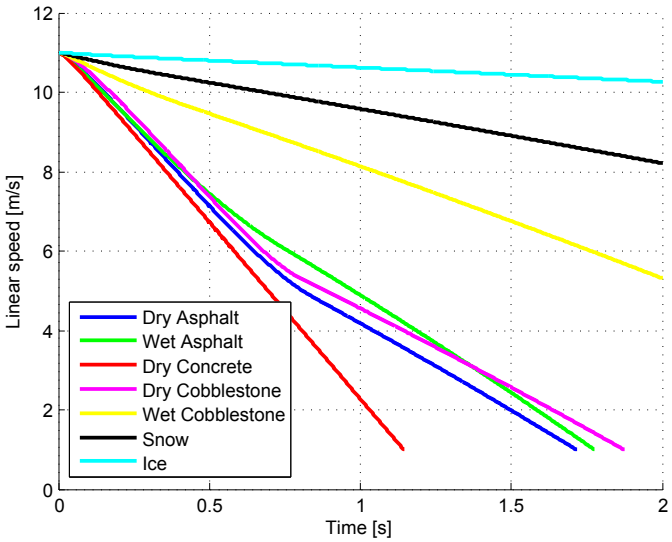

Figure 5.4: Linear speeds of the wheel in the various road conditions.

vehicle stops in about 1.2 seconds. On asphalt, concrete and dry cobblestone the decreasing rate of the speed is almost the same whilst on wet cobblestone, snow and ice the vehicles needs much more time to stops. This is caused by the braking torque used, that is almost optimal for some surfaces while causes wheel lock on the low adhesion ones. Running a longer simulation it turns out that in these cases the vehicle stops completely in more than 20 seconds.
In Figure 5.5 the behaviour of the angular velocity is shown. When the angular velocity reaches zero it means that the wheel is locked.

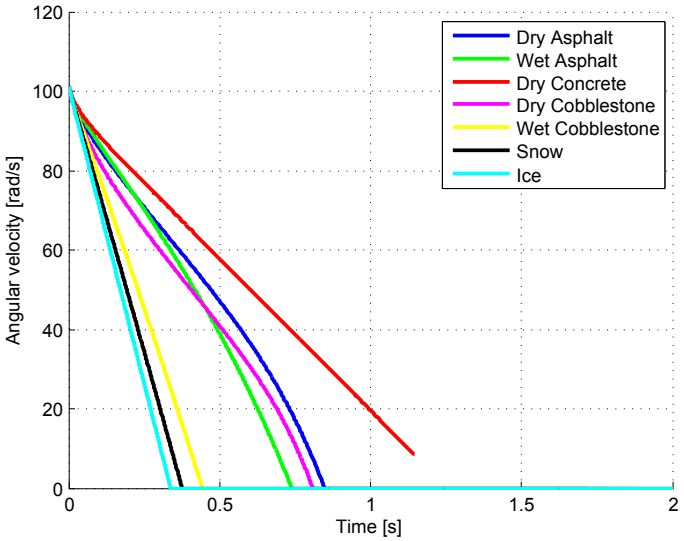

Figure 5.5: Angular velocities of the wheel in the various road conditions.

More interesting is Figure 5.6. It turns out that the vehicle needs less then 10

metres metres to stop if the braking is done on high adhesion surface whilst more than 100 on the ice because the braking torque is too high fur such a surface and cause the wheel locking.

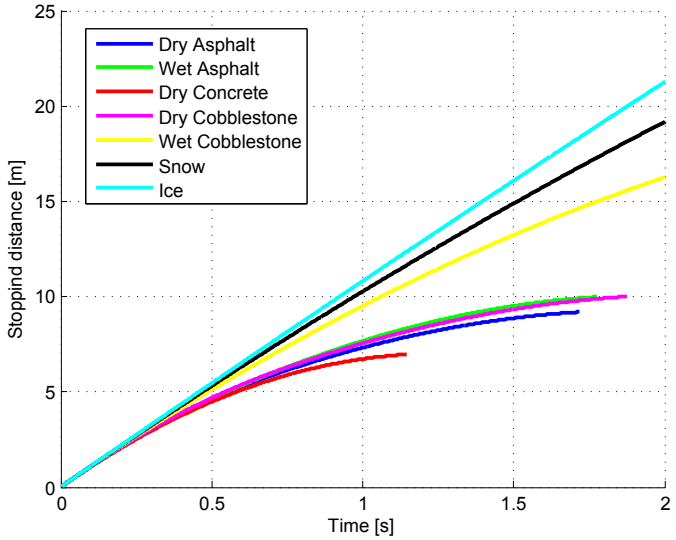

Figure 5.6: Stopping distances of the wheel in the various road conditions.

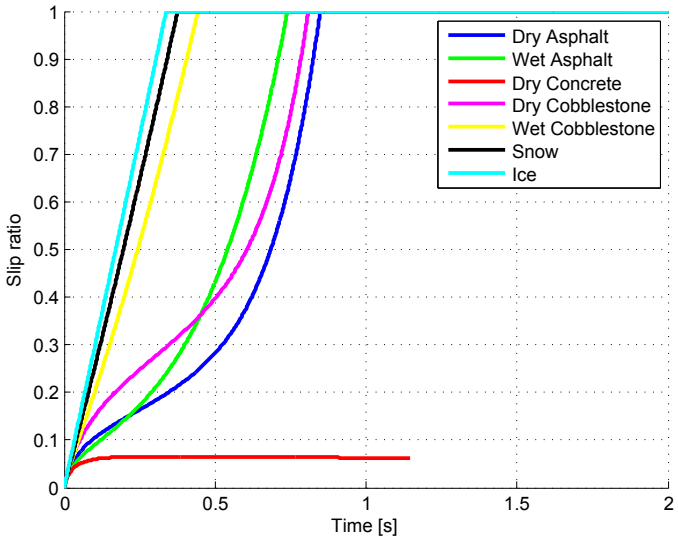

Figure 5.7: Slip ratios of the wheel in the various road conditions.

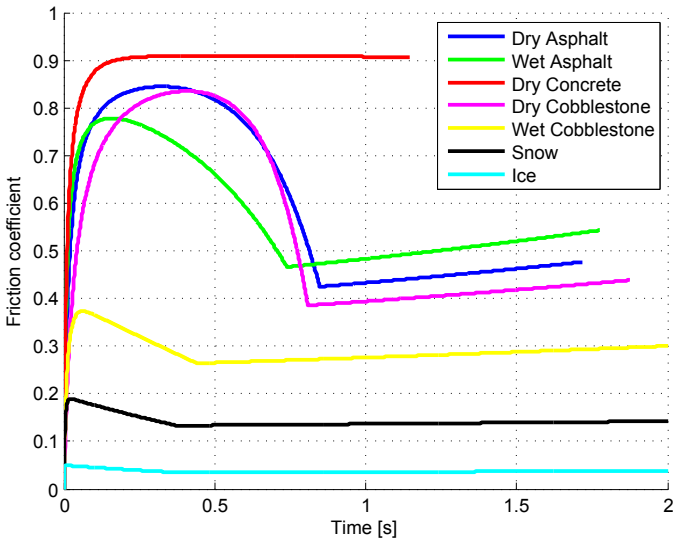

Figure 5.8: Friction coefficients of the wheel in the various road conditions.

5.1 Linearised Model and Dynamic Analysis

It is assumed [38] that the longitudinal dynamics of the vehicle (expressed by the state variable v) is much slower than the rotational dynamics of the wheel (expressed by the state variable λ or ω) due to large differences in inertia. Henceforth, v is considered as a slowly-varying parameter. Under this assumption, the second equation in 5.5 is neglected and the model reduces to a first order model of the wheel dynamics only:

$$\dot{\lambda} = -\frac{1}{v}\Big(\frac{1-\lambda}{m} + \frac{r^2}{J}\Big) mg\mu(\lambda) + \frac{r}{Jv} T_b \tag{5.6}$$

Throughout the chapter, the normalised linear wheel deceleration

$$\eta := -\frac{\dot{\omega} r}{g} \tag{5.7}$$

will sometimes be used. Observe that η is the linear deceleration of the contact point of the tyre, normalised with respect to the gravitational acceleration g. The first step in the analysis of the braking dynamics is the computation and discussion of the equilibrium points for the considered models, followed by their linearisation around the equilibrium points themselves. Based on the linearised models it will be also possible to carry out a dynamic analysis by means of the study of the system frequency response in order to investigate the model sensitivity to some vehicle parameters of interest.
To compute the equilibrium points, we set $\dot{v} = 0$ and $\dot{\omega} = 0$ starting from the equations 5.1. From

$$\begin{cases} rF_x - T_b = 0 \\ F_x = 0 \end{cases} \tag{5.8}$$

we obtain $F_x = 0$ thus $T_b = 0$. Recalling that $F_x = mg\,\mu(\lambda)$ and that $\mu(\lambda) = 0$ only for $\lambda = 0$, we have that the equilibrium is given by $\lambda = 0$ and $T_b = 0$. This corresponds to a constant-speed condition without braking but this equilibrium condition is trivial and meaningless for the design of a braking controller. The equilibrium points we are interested during braking are characterized by $\dot{\lambda} = 0$ (constant wheel slip ratio) and thus constant normalised linear wheel deceleration $\eta = \bar{\eta}$. According to the assumption of regarding the vehicle speed v as a slowly-varying parameter, the single car corner system can be modelled

using only the equation

$$\dot{\lambda} = -\frac{1}{v}\Big(\frac{1-\lambda}{m} + \frac{r^2}{J}\Big)mg\mu(\lambda) + \frac{r}{Jv}T_b \tag{5.9}$$

which can be rewritten by replacing v as $v = \frac{\omega r}{1-\lambda}$ (from the definition of the wheel slip ratio), obtaining

$$\dot{\lambda} = -\frac{1-\lambda}{J\omega}\big(\Psi(\lambda) - T_b\big) \tag{5.10}$$

where the function $\Psi(\lambda)$ is defined as

$$\Psi(\lambda) = \Big(r + \frac{J}{rm}(1-\lambda)\Big)F_z\mu(\lambda) \tag{5.11}$$

From the second last equation, it is obvious that the equilibrium points are characterized by

$$\overline{T_b} = \Psi(\overline{\lambda}) \tag{5.12}$$

Specifically, when the control input is constant, i.e., $T_b = \bar{T}_b$, the system exhibits the equilibrium points represented, in Figure 5.9, by the intersections between the curve $\phi(\lambda)$ and the constant value of the braking torque T_b.

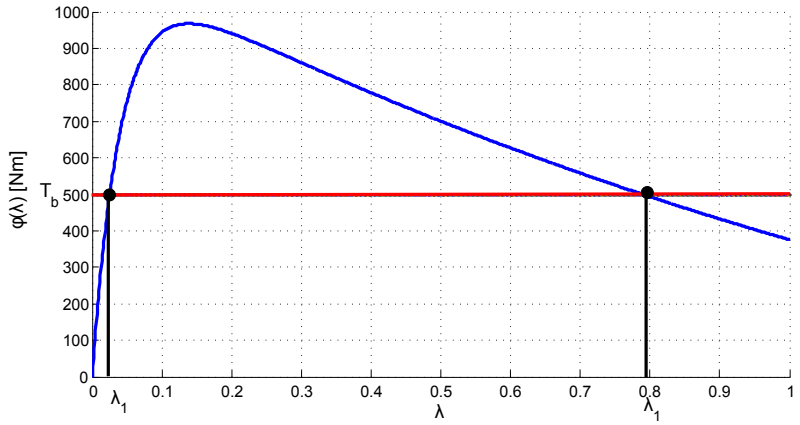

Figure 5.9: Equlibrium points for the singel-corner model in the (λ, T_b) plane (example with dry asphalt).

To summarise the system behaviour, one may note the following:

1. if $\bar{T}_b > \max\phi(\lambda)$, the system has no equilibrium points (recall that the model has been derived under the assumption that $\lambda \in [0, 1]$);

2. if $\bar{T}_b < \max\phi(\lambda)$ the system has at most two equilibria, namely $\bar{\lambda}_1$ and $\bar{\lambda}_1$ in Figure 5.9, where $\bar{\lambda}_1 < \bar{\lambda}_2$ are the two possibly coincident solutions

of

$$\overline{T_b} = \Psi(\overline{\lambda}) \tag{5.13}$$

Around one equilibrium point (which is characterized by $\overline{T_b}$, $\overline{\lambda}$, $\overline{\eta}$) are defined the following variables:

$$\delta T_b = T_b - \overline{T_b} \qquad \delta\lambda = \lambda - \overline{\lambda} \qquad \delta\eta = \eta - \overline{\eta}$$

To carry out the linearisation of the system, a crucial issue is how to consider and manage the dynamic dependency on the variable v: v is assumed to be a slowly-varying parameter since it is assumed that the longitudinal dynamics of the vehicle are much slower than the rotational dynamics of the wheel. As such, to linearise the model, the simplest approach is to neglect the second equation (vehicle dynamics) of system and work with the first-order model of the wheel dynamics.
Defining now

$$\mu_1(\lambda) := \frac{\partial\mu}{\partial\lambda}\Big|_{\lambda=\overline{\lambda}} \tag{5.14}$$

which represents the slope of the $\mu(\lambda)$ curve around an equilibrium point, the friction curve $\mu(\lambda)$ can now be expressed around the equilibrium point $\overline{\lambda}$ as

$$\mu(\lambda) \approx \mu(\overline{\lambda}) + \mu_1(\overline{\lambda})\delta\lambda$$

Linearising the wheel dynamics model

$$\dot{\lambda} = -\frac{1}{v}\Big(\frac{1-\lambda}{m} + \frac{r^2}{J}\Big)mg\mu(\lambda) + \frac{r}{Jv}T_b \tag{5.15}$$

assuming a constant speed value $v = \overline{v}$, we obtain

$$\delta\dot{\lambda} = \frac{F_z}{\overline{v}}\Big[\frac{\mu(\overline{\lambda})}{m} - \mu_1(\overline{\lambda})\Big(\frac{1-\overline{\lambda}}{m} + \frac{r^2}{J}\Big)\Big]\delta\lambda + \frac{r}{J\overline{v}}\delta T_b$$

In order to derive the transfer function, we consider δT_b as input and $\delta\lambda$ as output. Since the previous expression is linear, using the Laplace notation, finally we have

$$G_\lambda(s) = \frac{\frac{r}{J\overline{v}}}{s + \frac{F_z}{\overline{v}}\Big[\mu_1(\overline{\lambda})\Big((1-\overline{\lambda}) + \frac{mr^2}{J}\Big) - \mu(\overline{\lambda})\Big]} \tag{5.16}$$

In order to evaluate the transfer function $G_\eta(s)$ from δT_b and $\delta\eta$, we recall that the speed dynamics is given by

$$J\dot{\omega} = rF_z\mu\Big(\frac{v-\omega r}{v}, \theta_r\Big) - T_b$$

we can express η around one equilibrium point $\overline{\lambda}$ as

$$\delta\eta = \frac{r}{Jg}\delta T_b - \frac{r^2}{Jg}F_z\mu_1(\overline{\lambda})\delta\lambda \tag{5.17}$$

The transfer function is

$$G_\eta(s) = \frac{\frac{r}{Jg}\Big[s + \frac{F_z}{m\overline{v}}\Big(\mu_1(\overline{\lambda})(1-\overline{\lambda}) - \mu(\overline{\lambda})\Big)\Big]}{\Big[s + \frac{F_z}{m\overline{v}}\Big(\mu_1(\overline{\lambda})\big((1-\overline{\lambda}) + \frac{mr^2}{J}\big) - \mu(\overline{\lambda})\Big)\Big]} \tag{5.18}$$

5.2 Modelling the load transfer

In this section, the load transfer is discussed and modelled. With reference to wheeled vehicles, the load transfer is the measurable change of load borne by different wheels during acceleration (both longitudinal and lateral): of course, during braking a negative acceleration is generated. In the literature, the load transfer for the quarter of car model is defines as

$$\Delta_{lt} = \pm a\frac{h}{w_b}M \tag{5.19}$$

where Δ_{lt} is the weight variation to the wheel because of the load transfer, a is the acceleration (during braking is negative), h is the height of the center of gravity of the vehicle, w_b is the wheel base and M is the total mass of the vehicle. The sign in front of the acceleration depends if the wheel taken into account is a front or a rear one. In the first case, during a positive acceleration, the weight is transferred to the rear axle so the load in the front one decreases. While braking (negative acceleration) there is an increase of the load borne by the front wheels. In Table 5.2 the situation is summarized. In this work we refer to a front wheel of the vehicle and we focus on the braking dynamics: this means that the acceleration a is always negative and that while braking there

Axle	Acceleration	Sign in the formula
front	positive	-
front	negative	+
rear	positive	+
rear	negative	-

Table 5.2: Dynamic load transfer signs.

is a positive load transfer to the front axle, so the proper equation is

$$\Delta_{lt} = -a\frac{h}{w_b}M \tag{5.20}$$

In order to take into account the load transfer in the previous model, we need to add the amount of load transfer Δ_{lt} to the vertical load F_z borne by the single wheel:

$$F_{z_{ld}} = F_z + \Delta_{lt} \tag{5.21}$$

In the following table the parameters for the simulation are collected:

Parameter name	Parameter description	Value	Unit
h	height of the CoG	0.80	m
w_b	wheel base	0.26	m
M	vehicle total mass	1400	Kg

Table 5.3: Parameters for the load transfer simulation.

6

Conclusions and future recommendation

6.1 Simulink model of the ATV braking system

In Figure 6.2 the complete Simulink model is presented. This model has been built to be a basic simulator of the Polaris Ranger braking performances. As it has been explained in the previous chapters, some mathematical models have not been implemented because of the lack of parameters. In the following, the model is presented and described.

First of all, some external Matlab scripts allow to define the parameters of the system and the road conditions. Concerning the latter setting, six different configuration are available: dry or wet asphalt, dry concrete, dry or wet cobblestone, snow and ice.

The second block is the one that simulates the master cylinder build up pressure. Since the model derived in the second chapter has not been implemented in Simulink because of some discrepancies between the simulated and expected

behaviour (some more work has to be done in order to have a proper Simulink model), it implements simply the force-pressure relation inside the master cylinder, taking into account the mechanical multiplication ratio of the pedal. The situation is shown in Figure 6.1.

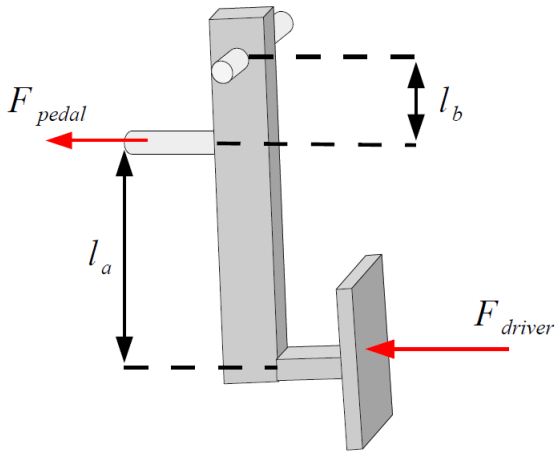

Figure 6.1: ATV Pedal Mechanical multiplication.

The mechanical multiplication factor is given by the ratio between the torque generated by the driver's input F_{driver} and the one transmitted to the master cylinder F_{pedal} thanks to the mechanical linkage of the pedal:

$$F_{pedal}\, l_b = F_{driver}\, l_a \tag{6.1}$$

Thus the multiplication factor is obviously

$$F_{pedal} = \frac{l_a}{l_b} F_{driver} \tag{6.2}$$

In the Polaris ranger, the multiplication is around 6.
The third block in the model, simulates some brake system capacitance in between the tandem master cylinder and the wheel cylinder. Physically, this correspond to the fact that after an initial flow without a pressure increase in the caliper's cylinder the pressure builds up. This is due to the expansion of the brake lines mostly. The phenomena is modelled with a pure time delay of $10\,ms$ and a first order transfer function.
the brake pressure-brake torque block implements the relation derived in the

second chapter between the brake fluid pressure inside the caliper's cylinder and the braking torque applied to the disk.
The block quarter of car model, implement the equations described in the fourth and fifth chapters about the tire-road interaction and the wheel dynamic.
Finally, a data collection block and some scopes allow to save the data to the Matlab workspace or check the simulation results while working with the model.

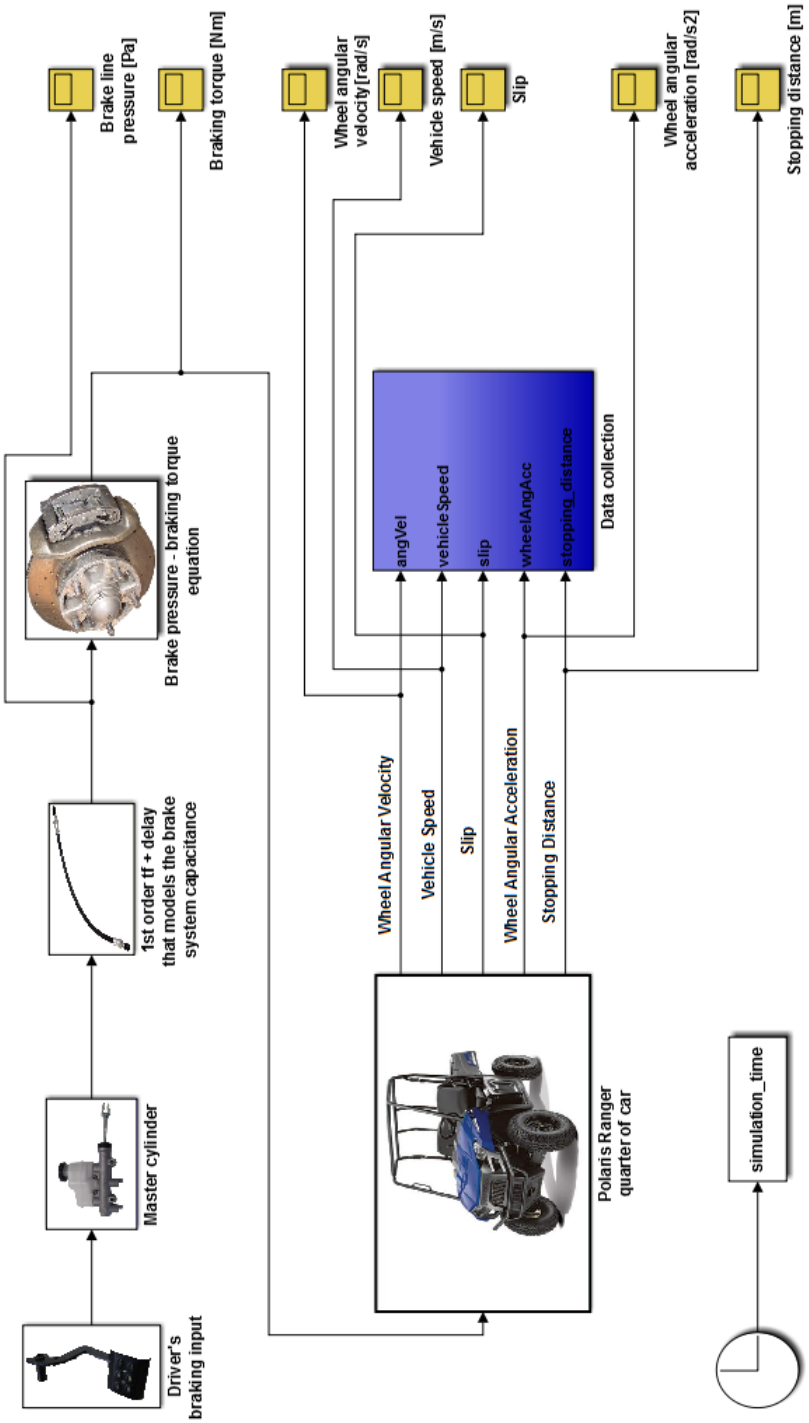

Figure 6.2: Overall view of the complete Simulink model.

6.2 Conclusions

This final project work belongs to a bigger project that aims to make the ATV Polaris ranger completely autonomous. The work will last several months and it is divided in several research group, each of them dealing with a different part of the vehicle (i.e. steering, vision systems, speed sensing, braking, ...). The focus of this work was the latter one.
The final project's target was providing an introduction to the anti-lock braking system features and characteristics and developing some mathematical models of the braking system in order to evaluate performance and providing some tools for simulations. Whenever it has been possible, the mathematical models have been implemented in Matlab/Simulink environment. In other cases, the lack of parameters and the need for some model identification made impossible to proceed with some simulations and only the theoretical model is given.
During the first part of the work, a deep literature research has been carried out, focusing on ABS technology, wheel slip and acceleration control techniques, hydraulic pressure modulations devices and actuators. The literature review in the first part show a wide range of possibilities in the ABS control, ranging from simple PID solution to highly non linear systems control techniques. One of the most promising is the sliding mode control because sliding mode controllers design provide a systematic approach to the problem of maintaining stability and consistent performance in the face of modelling imprecision and this is the case: modelling with high precision an hydraulic braking system is almost impossible so SMC offers a way to get good results without going uselessly to deep in mathematical analysis of the brake system', behaviour.
The second part has been involves with the analysis and modelling of the ATV braking system, starting from the quarter of car model to describe the wheel's dynamic during braking: equations of the vehicle's longitudinal velocity, wheel angular speed and acceleration and slip ratio have been derived. Furthermore, the interaction between tire and road has been investigated, providing the relationship between the friction available on different surfaces. Finally, the hydraulic part of the system has been studied: this part of the work ended up with the modelling of the tandem master cylinder-wheel cylinder dynamic model, nut the implementation in Simulink environment is not complete yet and can be carried out and integrated in the future.
A part of the work has been focused on the study of pressure modulation

devices: the most common and promising technology in this matter is the use of fast switching solenoid valves, to regulate the build up/hold/release pressure cycle. In this occasion, the model on a fast switching solenoid valve has been completed but not implemented because if the lack of parameters and the need of some hardware test to validate it.
All the models built compose a kind of vehicle braking performance simulator, presented in above: this model can for sure be integrated and improved, adding a the hydraulic model still and other features like load transfer during braking or a the suspension dynamic.
The simulations shows that the braking performance are highly dependent on road conditions and this suggest the use of anti-lock braking system technology in off-road vehicle like the ATV that has been the object of this work.

Further discussions

The work done during these months has been quite challenging for me: being in touch for the first time with the academic research approach is not easy for a student. Sometimes I spent even weeks on some papers or problems, trying to fix them proposing solutions. Sometimes the solution was the proper one, other times it has been necessary to leave that way starting on a new one. But probably this is the most challenging part of it: the researcher has first of all to figure out the problem to solve and then looking for a solution. Most of the times, the first part is the hardest. The latter one instead, is the one that need the most of the time.

6.3 Future recommendations

The main difficulty in this work has been the lack of a complete set of parameters in order to get better models for the simulations. This can be overcome thanks to a model identification procedure, done on the hydraulic system.
The big target is to make the ATV completely autonomous. The first step to proceed with the developing of the braking system is surely the installation of an hydraulic modulator between the tandem master cylinder and the brake lines. Once investigated the performance of the this device (like switching speed between increasing and decreasing pressure, delays, maximum pressure increase and decrease rate).

The actuation of the system can be done with an hydraulic cylinder pushing directly on the pedal, or even skipping the mechanical linkage and thus acting directly on the tandem master cylinder pushing rod.
The suggested layout is the one they proposed in [1]. There are two possibilities to control the vehicle braking performance: the first one is a slip controller (as they have done in [1]) and the second one is a wheel angular acceleration control. The main difference is the controlled variable. In the first case the slip can be calculated from the vehicle speed, which can be computed by average between the longitudinal speed of two wheels on the same diagonal (for example front left and rear right) and the wheels angular one which can be measured with a encoder. This calculation does not need any particular signal conditioning (like integration or derivation). The wheel angular acceleration control instead needs to get the wheel angular velocity and then to derive it to get the acceleration: this operation is sensible and may cause some numerical problems.
The slip control is better also because it can be implemented together with a road surface detector which is able to check for the surface condition variations providing a real time adaptation of the best slip reference value. Sliding mode control (SMC) is the suggested control technique because it can cope for the systems modelling uncertainties: together whit the SMC algorithm, it is suggested to modify it (refer to [1]) in order to avoid the chattering problem due to the discontinuity in the control signal.

Bibliography

[1] Ming-chin Wu, Ming-chang Shih *Simulated and experimental study of hydraulic anti-lock braking system using sliding-mode PWM control*, Department of Mechanical Engineering, National Cheng Kung University, Tainan, Taiwan, ROC, 2001

[2] Bo-Rong Liang, Wei-Song Lin, *A new Slip Ratio Observer and Its Application in Electric Vehicle Wheel Slip Control*, IEEE International Conference on Systems, Man and Cybernetics, 2012

[3] J. Song, H. Kim and K. Boo, *A study on an Anti-Lock Braking System Controller and Rear-Wheel Controller to Enhance Vehicle Lateral Stability*, Proceedings of the Institution of Mechanical Engineers, Part D: Journal of Automobile Engineering, Vol. 221 No. 7, 2007, pp. 777- 787

[4] F. Jiang, *An Application of Non-linear PID Control to a Class of Truck ABS Problems*, Proceedings of the 40th IEEE Conference on Decision and Control, Orlando, 2000, pp. 516-521

[5] M. Tanellia, A. Astolfi and S. M. Savaresi, *Robust Non-linear Output Feedback Control for Brake by Wire Control Systems*, Automatica, Vol. 44, No. 4, 2008, pp. 1078-1087

[6] R. Freeman, *Robust Slip Control for a Single Wheel*, University of California, Santa Barbara, 1995.

[7] Y. Liu and J. Sun, *Target Slip Tracking Using Gain-Scheduling for Braking Systems*, Proceedings of the 1995 American Control Conference, Seattle, 1995, pp. 1178-1182.

[8] J. Lüdemann, *Heterogeneous and Hybrid Control with Application in Automotive Systems*, Ph.D. dissertation, Glasgow University, 2002.

[9] S. Drakunov, Ü. Özgÿner, P. Dix, and B. Ashrafi, *ABS Control Using Optimum Search via Sliding Modes*, IEEE Transactions on Control Systems Technology, Vol. 3, 1995, pp. 79-85.

[10] M. Schinkel and K. Hunt, *Anti-lock Braking Control Using a Sliding Mode Like Approach*, Proceedings of the 2002 American Control Conference, Anchorage, 2002, pp. 2386-2391

[11] M. C. Wu and M. C. Shih, *Hydraulic Anti-Lock Braking Control Using the Hybrid Sliding-Mode Pulse Width Modulation Pressure Control Method*, Proceedings of the Institution of Mechanical Engineers, Vol. 215, 2001, pp. 177-187.

[12] C. Ünsal and P. Kachroo, *Sliding Mode Measurement Feedback Control for Anti-lock Braking Systems*, IEEE Transactions on Control Systems Technology, Vol. 7, No. 2, March 1999, pp. 271-281.

[13] R.-G. Wang, Z.-D. Liu and Z.-Q. Qi, *Multiple Model Adaptive Control of Anti-lock Brake System via Backstepping Approach*, Proceedings of 2005 International Conference on Machine Learning and Cybernetics, Guangzhou, 2005, pp. 591-595.

[14] T. A. Johansen, J. Kalkkuhl, J. Lüdemann and I. Petersen, *Hybrid Control Strategies in ABS*, Proceedings of the 2001 American Control Conference, Arlington 2001, pp. 1704-1705.

[15] J. C. Gerdes, A. S. Brown and J. K. Hedrick, *Brake System Modeling for Vehicle Control*, Proceedings In-ternational Mechanical Engineering Congress and Exposition, San Francisco, 1995, pp. 4756-4763.

[16] D. Cho and J. K. Hedrick, *Automotive Powertrain Modelling for Control*, Transactions ASME Journal of Dy-namic Systems, Measurements and Control, Vol.111, No.4, December 1989, pp. 568-576.

[17] E. Kayacan and O. Kaynak, *A Grey System Modeling Approach for Sliding Mode Control of Antilock Braking System*, IEEE Transactions On Industrial Electronics, Vol. 56, No. 8, August 2009, pp. 3244-3252.

[18] W. Ting, J. Lin, *Nonlinear Control Design of Anti-lock Braking system Combined with Active Suspensions*, Technical report of Department of Electrical Engineering, National Chi Nan University, 2005.

[19] B. Ozdalyan, *Development of A Slip Control Anti-Lock Braking System Model*, International Journal of Auto-motive Technology, Vol. 9, No. 1, 2008, pp. 71-80.

[20] A. B. Will and S. H. Zak, *Antilock Brake System Mod-elling and Fuzzy Control*, International Journal of Vehicle Design, Vol. 24, No. 1, 2000, pp. 1-18.

[21] J. R. Layne, K. M. Passino and S. Yurkovich, *Fuzzy Learning Control for Antiskid Braking Systems*, IEEE Transactions on Control Systems Technology, Vol. 1, No. 2, 1993, pp. 122-129.

[22] G. F. Mauer, *A Fuzzy Logic Controller for an ABS Braking System*, IEEE Transactions on Fuzzy Systems, Vol. 3, No. 4, 1995, pp. 381-388.

[23] W. K. Lennon and K. M. Passino, *Intelligent Control for Brake Systems*, IEEE Transctions on Control Systems Technology, Vol. 7, No. 2, 1999, pp. 188-202.

[24] C. Unsal and P. Kachroo, *Sliding Mode Measurement Feedback Control for Anti-lock Braking Systems*, IEEE Transactions on Control Systems Technology, Vol. 7, No. 2, 1999, pp. 271-280.

[25] S.W. Kim and J.J. Lee, *Design of a Fuzzy Controller with Fuzzy Sliding Surface*, Fuzzy Sets and Systems, Vol. 71, No. 3, 1995, pp. 359-369.

[26] C. M. Lin, C. F. Hsu, *Self-Learning Fuzzy Slid-ing-Mode Control for Antilock Braking Systems*, IEEE Transactions On Control Systems Technology, Vol. 11, No. 2, 2003, pp. 273-278.

[27] J. R. Laynet, K. M. Passinot and S. Yurkovich, *Fuzzy Learning Control for Anti-Skid Braking Systems*, IEEE Transactions on Control Systems Technology, Vol. 1, No. 2, 1993, pp. 122-129

[28] J. Laynet and K. M. Passino, *Fuzzy Model Reference Learning Control for Cargo Ship Steering*, IEEE Control Systems Magazine, Vol. 13, No. 6, September 1992, pp. 23-24.

[29] Bosch GmbH, *Automotive Brake Systems*, 1996

[30] Bosch GmbH, *Automotive Brake Systems*, SAE International 1996

[31] Bosch GmbH, *Driving Safety Systems 2nd edition*, SAE International 1999

[32] Bosch GmbH, *Safety, Comfort and Convenience Systems*, 2006

[33] Y. K. Chin, W. C. Lin and D. Sidlosky, *Sliding-Mode ABS Wheel Slip Control*, Proceedings of 1992 ACC, Chicago, 1992, pp. 1-6

[34] *Development of a slip control anti-lock braking system model.* International Journal of Automotive Technology Volume 9, Issue 1 , pp 71-80

[35] M. Taghizadeh, A. Ghaffari, F. Najafi, *Modelling and identification of a solenoid valve for PWM control applications.*, C.R Mecanique, pp. 131-140, 2009

[36] E.E. Topcu, I. Yuksel, Z. Kamis, Development of electro-pneumatic fast switching valve and investigation of its characteristics, Mechatronics, pp.365?378, 2006

[37] Ayman A. Aly, El-Shafei Zeidan, Ahmed Hamed, Farhan Salem, *An Antilock-Braking Systems (ABS) Control: A Technical Review* Intelligent Control and Automation, 2011, 2, 186-195

[38] Tor A. Johansen, Idar Petersen, Jens Kalkkuhl, Jens Ludemann, *Gain-Scheduled Wheel Slip Control in Automotive Braking Systems*, IEEE Transaction on Control Systems Technology, Vol. 11, No.6, 6, November 2003

[39] R. Johansson and A. e. Rantzer, *Nonlinear and Hybrid Systems in Automotive Control.* London, Springer-Verlag, 2003

[40] Rajesh Rajamani, *Vehicle Dynamics and Control*, Springer, 2006

[41] Mathieu Gerard , William Pasillas-LÃ©pine , Edwin de Vries & Michel Verhaegen *Improvements to a five-phase ABS algorithm for experimental validation*, Vehicle System Dynamics: International Journal of Vehicle Mechanics and Mobility, 50:10, 1585-1611,, Taylor & Francis, 2012

A

Modelling a fast switching solenoid valve

A part the work have been involved with the modelling of a fast switching solenoid valve, in order to provide a mathematical model to use for simulations. Because the model, to be accurate, needs to be tested and identified on the hardware, the derived equations are still reported below for future usage.

Solenoid valves are the most frequently used control elements in fluid-dynamics. Their tasks are to shut off, release, dose, distribute or mix fluids. They are found in many application areas. Solenoids offer fast and safe switching, high reliability, long service life, good medium compatibility of the materials used, low control power and compact design. Figure A1 depicts the basic components of a solenoid valve. The valve shown is a normally-closed (NC) solenoid operated 2/2 directly-acting valve. The main components are:

1. Valve body;
2. Inlet port;
3. Outlet port;

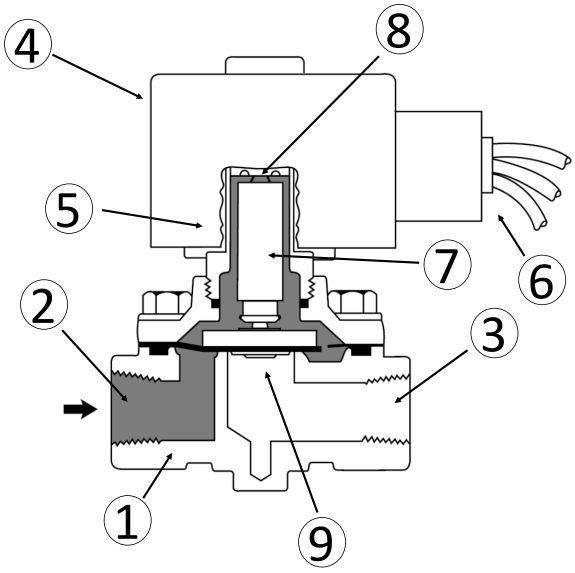

Figure A1: Solenoid valve general layout.

4. Coil/Solenoid;
5. Coil windings;
6. Lead wires;
7. Plunger;
8. Spring;
9. Orifice.

The valve is a solenoid operated on?off, 2/2 (one inlet port and one outlet port), spring return with a disc element. The valve consists of two major parts. The upper part (4) houses an electromagnetic core with a coil and provides a drain connection. The lower one (1) forms a disc chamber and provides a pressure connection. The disc forms a seating type of valve and also constitutes a moving part of magnetic circuit. It moves between a nozzle and a preloaded spring under resultant force of magnetic, spring and flow forces. The diameter of the disc chamber is slightly less than the diameter of the magnetic core to prevent the magnet being pulled into the chamber by magnetic force. The fluid controlled by the solenoid valve enters the valve through the inlet port (2). In order to exit the valve through the outlet port (3), the fluid has to pass through the orifice (9) that is closed and opened by the plunger (7). The valve is arranged to be normally closed by the preloaded spring acting on the

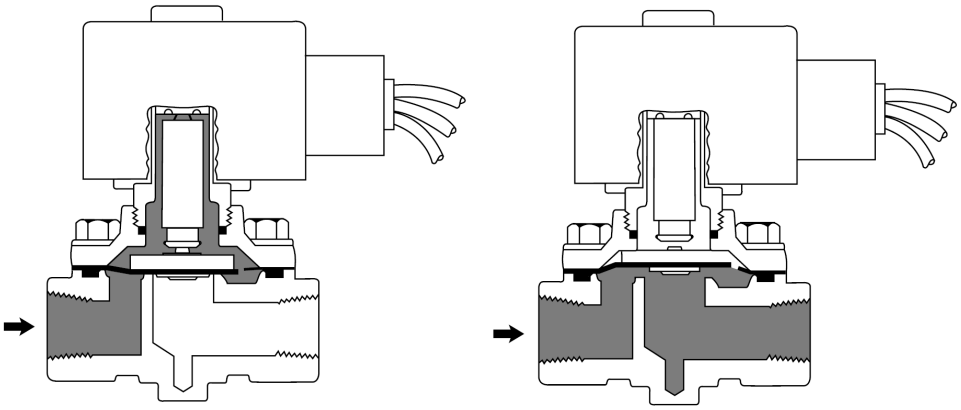

Figure A2: Solenoid valve not energized, the orifice is close (left) and Solenoid valve energized (the orifice is open)

plunger keeping the orifice closed against the pressurized flow path. When the coil is energized, magnetic attraction force pulls the plunger against spring force and the valve opens and the fluid flows through the flow path of the valve. As depicted in Figure A2, when the coil is not energized, the the pre-loaded spring pushes the plunger against the coil in order to close it. Once a voltage is applied to the coil instead, the resulting electromagnetic force pulls up the plunger, opening the orifice and allowing in this way the fluid to pass through the valve. In order to model the behaviour of this device, it it useful to divide it into subsystems,as in Figure A3.

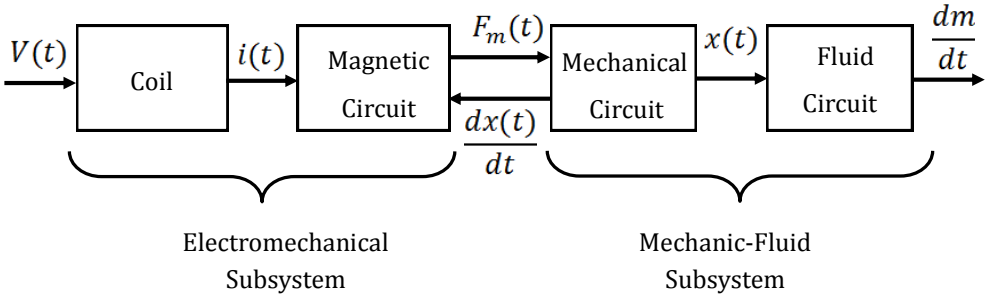

Figure A3: Solenoid valve block diagram.

Electromagnetic Subsystem

The electromagnetic sub-system consists of an electrical and magnetic circuit. The magnetic circuit consists of a fixed core surrounded by the coil turns, and a moving part which is connected to the spool and moves with the spool under

the effect of the exerted magnetic force. The electrical circuit is the coil which is represented with an ideal inductance L in series with a resistance R of the coil. Thus the equations for the electromechanical sub-system can be written applying Kirchhoff?s law:

$$V(t) = Ri(t) + \frac{d}{dt}L(t)i(t) \; = \; Ri(t) + L(t)\frac{d}{dt}i(t) + i(t)\frac{d}{dt}L(t) \tag{A1}$$

where $V(t)$ is the input voltage and $i(t)$ is the current flowing through the circuit. In order to find out the equation for the inductance $L(t)$ the equivalent length of the total magnetic circuit l_{eq} is defines as [35]

$$l_{eq} = l_c + \frac{\mu_c}{\mu_0} l_g \tag{A2}$$

where l_c is the length of the magnetic circuit inside the core, l_g is the length of the magnetic circuit in the air, μ_c is the magnetic permeability of the core and μ_0 the one of the air. If $x(t)$ is the spool position, then l_{eq} can be expressed as

$$l_{eq} = l_c + 2\mu_r(x_t - x(t)) \tag{A3}$$

where $\mu_r = \frac{\mu_c}{\mu_0}$ is the relative permeability of the core and x_t is the total air gap that includes holding gap and travelling gap of the spool. For this circuit, the electromotive force can be stated as

$$Ni(t) = H_c l_c + H_g l_g = H_c l_e q \tag{A4}$$

where N is the number of coil turns, and H_c and H_g are the magnetic field intensity in the core and in the air gap respectively. Now, combining the previous equations with the fundamentals magnetic relations

$$\begin{cases} H_c = \frac{B}{\mu_c} = \frac{\varphi(t)}{A_e \mu_c} \\ Li(t) = N\varphi(t) \end{cases} \tag{A5}$$

in which $\varphi(t)$ is the magnetic flux intensity, A_e is the effective cross-sectional area of the magnetic circuit and B is the magnetic flux density, the variable inductance $L(t)$ results

$$L(t) = \frac{N^2 A_e \mu_c}{l_{eq}} = \frac{N^2 A_e \mu_c}{l_c + 2\mu_r(x_t - x(t))} \tag{A6}$$

and its first derivative is

$$\frac{d}{dt}L(t) = \frac{2\mu_r L^2(t)\dot{x}(t)}{N^2 A_e \mu_c} \tag{A7}$$

From the Kirchhoff' s equation stated at the beginning, we finally have the following

$$\frac{d}{dt}i(t) = \frac{1}{L(t)}\Big(V(t) - Ri(t)\Big) - \frac{2\mu_r L^2(t)\dot{x}(t)i(t)}{N^2 A_e \mu_c} \tag{A8}$$

The last equation is that one which relates the magnetic attraction force $F_m(t)$ with the current:

$$F_m(t) = \frac{L^2(t)i^2(t)}{N^2 A_e \mu_0} \tag{A9}$$

Mechanic Subsystem

The mechanical subsystem consists basically of a mass, spring and damper under the effect of magnetic and pressure forces. According to Newton?s second law

$$m_s\frac{d^2x(t)}{dt^2} + b\frac{dx(t)}{dt} + k(x(t) + \delta) = F_m(t) + Fprs(t) \tag{A10}$$

where m_s is the mass of the spool, b is the damping coefficient, k is the spring coefficient of the valve, δ is the spring pre-tension and $F_{prs}(t)$ is the pressure force affected on the spool. In order to compute the pressure force acting on the spool, let's consider Figure A4. The pressure force can be simply approximated by

$$F_{prs}(t) = P_{sup}(t)d_1 + P_{out}(t)d_2 \tag{A11}$$

where P_{sup} and P_{out} are the supply pressure and the outlet pressure.

Fluid Subsystem

The electromagnetic and mechanical parts of the valve are used to control the fluid flow through the valve orifice by controlling the spool position. The orifice equation for turbulent flow is used to describe the air flow through the valve [36]. This equation consists of two different static functions for subsonic and choked (sonic) flow regimes. As the fluid in the valve and in the pneumatic system is compressible, when the ratio of the supply pressure (P_{sup}) to the downstream pressure (P_{out}) is larger than a critical value, the flow regime is subsonic and the mass flow depends nonlinearly on both pressures. Whereas,

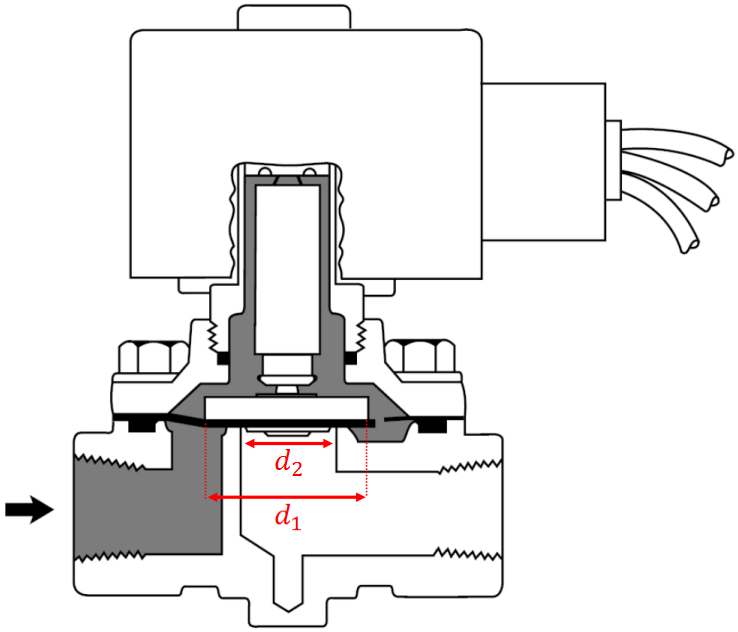

Figure A4: Solenoid valve orifice dimensions.

when the pressure ratio is smaller than the critical ratio, the flow attains sonic velocity and depends linearly on the upstream pressure. In both cases, the fluid mass flow depends linearly on spool position. The standard equation for mass flow rate through an orifice is given by

$$\frac{dm}{dt} = \begin{cases} 0.0405 C_d A_v \frac{P_{sup}}{\sqrt{T}} & \text{if } \frac{P_{out}}{P_{sup}} = 0.5280 \\ C_d A_v \frac{P_{sup}}{\sqrt{T}} \left[\frac{2\gamma}{R(\gamma-1)} \left(\left(\frac{P_{out}}{P_{sup}}\right)^{\frac{2}{\gamma}} - \left(\frac{P_{out}}{P_{sup}}\right)^{\frac{\gamma+1}{\gamma}} \right) \right]^{\frac{1}{2}} & \text{if } \frac{P_{out}}{P_{sup}} > 0.528. \end{cases} \tag{A12}$$

where C_d is the discharge coefficient, A_v is the effective cross-sectional area of fluid flow path, and T is the upstream stagnation temperature.

B

Automotive safety technology overview

Figure A1: Automotive safety technology.